OMICS eBooks International

Chemical Bath Deposition of Crystalline Cu_4SnS_4 Thin Films

Edited by
Dr. Ho Soon Min

Chemical Bath Deposition of Crystalline Cu_4SnS_4 Thin Films

Edited by: Dr. Ho Soon Min

ISBN: 978-1-63278-006-5

DOI: 10.4172/978-1-63278-006-5-007

Published Date: November 2017

Printed Version: November 2017

Published by **OMICS International eBooks**

731 Gull Ave, Foster City, CA 94404, USA.

A free online edition of this book is available at www.esciencecentral.org/ebooks

Additional hard copies can be obtained from orders @ www.esciencecentral.org/ebooks

Preface

The present book focuses on the preparation of copper tin sulphide thin films by using chemical bath deposition method. The advantage of this deposition method is that it needs in it's the simplest form only solution and substrate. In other words, this method is one of the cheapest methods to deposit thin films. In this work, thin films will be prepared under various deposition conditions such as bath temperature, deposition time, complexing agent, concentration of solution and pH. Characterization of obtained films will be investigated using X-ray diffraction, atomic force microscopy, UV-Visible spectrophotometer and energy dispersive X-ray analysis. Lastly, this book will support the students, researchers and all the persons interested towards the study in metal chalcogenide thin films.

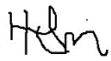

Signature

About author

Associate professor Dr HO SOON MIN is presently working at Faculty of Information Technology, Mathematic and Sciences, INTI International University, Malaysia. He received his Ph.D in Materials Chemistry at University Putra Malaysia. He taught academic courses in physical chemistry, general chemistry, chemistry & society since last seven years. His research areas include green chemistry, semiconductor, Nano materials, applied chemistry, activated carbon and thin film solar cell. He has authored or co-authored for more than 130 articles in international referred journals and book chapter as well. He was appointed as journal reviewer, editorial board member, thesis evaluator and head of center of applied chemistry and green chemistry.

OMICS eBooks International

Acknowledgements

I am thankful to all the persons/colleagues/university staff that supported me on this book. Also, I am grateful to the OMICS International eBooks Team in the publishing of this book.

Introduction to the eBook

The chapters in this eBook include topics from the thin films, solar cells, thin film deposition method, influence of optical, structural, morphological and compositional properties of films under various deposition conditions. On these topics, a compilation of all the relevant information/experimental results covered in each topic and subtopic was held. Also, references are provided for readers such as academician, students, and researcher who wish to delve deeper into some of the issues. This book will be very useful as networking and literature citation about metal chalcogenide thin films.

List of the contents

OMICS eBooks International

Chemical Bath Deposition of Crystalline Cu4SnS4 Thin Films

Ho Soon Min*

Faculty of Information Technology Mathematic & Science, INTI International University, Malaysia.

***Corresponding author:** Faculty of Information Technology Mathematic & Science, INTI International University, Malaysia, Tel: 606-7982000; E-mail: soonminho@yahoo.com

Introduction

Solar energy is radiant light and heat from the Sun. It is a free, clean energy and inexhaustible resource. Solar cell is consisting of two types of semiconductors, namely *p*-type and *n*-type materials. When sunlight is absorbed by these materials, the solar energy knocks electrons loose from their atoms, allowing the electrons to flow through the material to produce electricity. A few decades ago, the search for thin film materials for solar energy conversion has been identified by many researchers all over the world. The optimum band gap value, high absorption coefficient and the interesting structural properties satisfy most of the criterion to make them candidate in the low cost thin film solar cell technology.

Silicon Based Solar Cells

The most important material for solar cells is still silicon due to availability, no toxicity, long lifetime and sustainability. Up-to-date, there are approximately 90% of solar cells modules are based on crystalline silicon technology. The biggest global producers of crystalline silicon based solar cells such as Suntech Power, Q-cell, JA Solar, Tianwei Yingli SC, Motech Industustries, SunPower, CSI Canadian Solar, Gimtech Energy, Trina Solar and Sharp Corporation.

Solar Star project is the largest solar power plant. The plant produces 579MW capacity and generates enough electricity to power around 255000 homes. The site uses 1.7 million Sun Power made monocrystalline silicon modules on single axis trackers. The Erlasee Solar Park is located in Germany. This solar plant is an 11.4 megawatt station and uses 1464 double axis solar trackers. Each tracker shoulders twelve conventional solar panels made of crystalline silicon.

Thin Film Based Solar Cells

There are two types of thin film namely, cadmium telluride (CdTe) and copper indium gallium diselenide (CIGS) solar panels on the market today. This type of solar cells is potentially cheaper than traditional panels but less efficient. Companies involved in CdTe and CIGS panel production including Siva Power, Antec solar, Advanced Solar Power, CTF solar, Solar Frontier, Global Solar Energy, Ascent Solar, Solar Power, First Solar, Calyxo, Dmsolar and Nexcis.

Desert Sunlight Solar Farm is located in California. This farm is built using 8 million plus cadmium telluride solar modules. Energy produced (550 MW) serves about 160000 homes in the country. The Agua Caliente Solar Project is 290 MW power plant and is located in Arizona. Thin film technology based cadmium telluride photovoltaic panels from the developer. It was completed in 2014 and powers 100000 homes.

Polymer Solar Cells

Organic solar cells are flexible solar cell, prepared from earth abundant materials and inexpensive polymer hold the promise of capturing solar power in a low cost, light in weight and environmentally friendly way. This type of solar cell can also display transparency, suggesting applications in glass, rods, cabinet, windows, flexible electronics and walls. The researchers from University of California, Los Angeles have developed a new transparent polymer solar cell to produce electricity while still allowing people to see outside. They explain that this solar cell produces energy by absorbing mainly infrared light; the photoactive plastic cell is nearly 70% transparent to the human eye.

Dye Sensitized Solar Cell

A dye sensitized solar cell (DSSC) is a low cost solar cell belonging to the group of thin film solar cells and was developed by Gratzel and his team. The working of the DSSC is entirely different from other types of solar cells. Generally, it is based on a semiconductor produced between a photo sensitized anode and an electrolyte, a photo electrochemical system. The efficiency of DSSC has continued to increase in the last 20 years, with a confirmed record of 14.1%, was achieved by Gratzel and his team. DSSC has many advantages such as low light performance, variety of substrate, higher temperature performance, ecologically friendly solar and optimized performance.

Thin Film Deposition Methods

There is several deposition techniques have been used in order to prepare thin films. For example, spray pyrolysis, pulsed electro deposition method, chemical bath deposition, electro deposition, chemical vapor deposition, brush plating, successive ionic layer adsorption and reaction, magnetron sputtering, dip sol method, vacuum evaporation, and thermal evaporation. Among these methods, chemical bath deposition method is more attractive since this method offers the advantages of simple, low-cost and convenient for large area deposition at low temperature. In most of the experimental approaches, substrates are immersed in an aqueous solution (alkaline or acidic solution) containing the chalcogenide source, metal ion and complexing agents. In chemical bath deposition, a complexing agent is used to bind the metallic ions to avoid the homogeneous precipitation of the corresponding compound. The formation of a complex ion is essential to control the rate of the reaction and to avoid the immediate precipitation of compound in the solution. When the solution is saturated, the ionic product is equal to solubility product. As the ionic product slowly exceeds the solubility product the solution becomes supersaturated and precipitation occurs. The deposition begins with nucleation phase followed by growth phase in which the thickness of film increases with duration up to the terminal phase where film depletion into constituent ions occur after a certain time.

Power Conversion Efficiency in Thin Films

There are many researchers have reported the photovoltaic characteristics in their experiments. The obtained thin films were used as absorbers materials during the fabrication of heterojunction solar cell. Power conversion efficiency of films was defined as the ratio of power produced by the fabricated solar cell to the incident sunlight energy into the cell per time. The overall power conversion efficiency ranges from 0.12 – 13% as reported by them

[1-10]. Furthermore, researchers have suggested that the solar cell device efficiencies of less than 3% are too low for commercialization and need to be improved.

Binary Thin Films

Binary thin films consist of two different elements. In the past few decades, there were a number of reports on the properties of thin films prepared by different deposition methods [11-19]. They have a wide range of applications. These materials were used as optical mass memories, solar cells, hologram recording, solar selecting coatings, sensor devices, laser devices, photo-luminescent and electro-luminescent devices. They are attracting considerable attention due to many reasons such as simple, inexpensive and convenient for large area deposition process. Generally, thin binary films will be deposited onto various substrates such as soda lime glass, indium tin oxide glass, stainless steel, and microscope glass slide.

Ternary Thin Films

Deposition of ternary metal sulfide films, selenide films and telluride films has been reported by many scientists [20-36]. The precursors used were metal ions, chalcogenide ions, and complexing agent. Variation in structure, morphology and composition of thin films was observed at different deposition conditions.

Quaternary Thin Films

In recent years, quaternary thin films [37-48] such as I-II-IV-VI semiconductor have attracted attention. For example, most of the researchers have prepared Cu_2ZnSnS_4 thin films onto different substrates for the use as the photo absorber in photovoltaic cells. Due to the fact that these materials are low cost, direct band gap, high optical absorption coefficient and non-toxic constituents. In order to improve the performance of these films, efforts should be committed to the development of the approaches for producing pure phase. Also, another suggestion was the detection techniques of secondary phases produced during the deposition of the films.

Penternary Thin Films

Solution deposition method, electrodeposition method, physical vapor deposition and evaporation technique have been used to prepare $Cu(In,Ga)(S,Se)_2$ and $Cu_2ZnSn(SSe)_4$ thin films. Researchers found that these films could be employed as absorbing materials in photovoltaic application. For example, the power conversion efficacy values ranges from 6.03% to 12.4% for these materials. The competitiveness of production cost and band gap energy matching solar spectrum lead to chalcogenide materials are attractive for solar energy conversion. Currently, the types of research done by various scientists [49-53] are mostly related to the investigation of materials properties especially suited to solar cell applications.

Materials and Methods

Chemicals Used

All the chemicals used for the deposition were analytical grade without further purification. The chemicals include copper sulfate ($CuSO_4$), tin chloride ($SnCl_2$), sodium thiosulfate ($Na_2S_2O_3.5H_2O$), potassium hexacyanidoferrate (II) ($K_4[Fe(CN)_6]$, Potassium hexacyanoferrate (III) ($K_3[Fe(CN)_6]$, sodium hydroxide, ethanol (C_2H_5OH) and hydrochloric acid. All the solutions were prepared using deionised water from Millipore Alpha-Q System.

Characterization tools

The number of metal chalcogenide thin films used in solar cell and optoelectronic applications has rapidly increased in the past two decades. There are many tools will be used in order to study the physical, electrical, optical and chemical behaviors of thin films as reported by many researchers [54-80].

X-ray diffraction (XRD)

X-ray diffraction technique was used to investigate the structure of obtained films. The position and the intensities of the peaks are used for identifying the underlying structure of the materials. The patterns obtained from experimental samples were compared to Joint Committee on Powder Data Standards (JCPDS) data to identify crystalline phases. A SCINTAG XRD 2000 X-ray diffractometers using CuK_{α} (λ=1.5418Å) was used for this study. The scanning rate was set to 2°/min with a 0.02° step size and the range from 20° to 60°. The relationship describing the angle at which a beam of X-rays of a particular wavelength diffracts from a crystalline surface is known as Bragg's Law.

$$n\lambda = 2dsin\theta \quad (1)$$

λ = wavelength of the X-ray

θ = diffraction angle

n= integer representing the order of diffraction peak

d = interplanar spacing generating the diffraction

Atomic force microscopy (AFM)

The Atomic Force Microscopy (AFM) was performed on the sample to analyze the surface morphology of thin films from angstroms (Å) to 100 μm. In this study, AFM was carried out using a Q–Scope 250 (Quesant Instrument Corporation) which operating in contact mode with a commercial Si_3N_4 cantilever. It is the most popular Quesant model, primarily used in stand-alone applications. It is equipped with PC-based video subsystem using a CCD camera for 90° tip and sample viewing and a manual X-Y translation stage for sample positioning. It also provides a three-dimensional surface profiles.

UV-Visible spectrophotometer

Ultraviolet Visible spectroscopy involves the spectroscopy of the photons and spectrophotometry. It uses light in the visible and ultraviolet region. In this region of energy space molecules undergo electronic transitions. In this study, Perkin Elmer UV-Vis Spectrophotometer Lambda 20 has been used for investigation of the absorption spectra of the samples. The indium tin oxide coated glass substrate was placed in the reference path while the deposited films in the sample radiation path. The optical properties of films deposited on ITO glass substrates were investigated from the absorption measurements in the range of 300-800 nm. The band gap energy and transition type were derived from mathematical treatment with the following relationship for near-edge absorption

$$A = \frac{k(h\upsilon - E_g)^{n/2}}{h\upsilon} \quad (2)$$

Where A is absorbance, E_g is band gap energy, h is Plank's constant ($6.63x10^{-34}$), υ is frequency in Hertz, k equals a constant value, n carries the value of either 1 or 4. The arrangement of the equation (1) gives the following equation:

$$(Ah\upsilon)^{2/n} = k(h\upsilon - E_g) \quad (3)$$

For a direct transition when n=1, the equation (2) becomes

$$(Ahv)^2 = k(hv - E_g) \quad (4)$$

For an indirect transition when n=4, the equation (2) becomes

$$(Ahv)^{1/2} = k(hv - E_g) \quad (5)$$

The data were used to plot a graph of $(Ahv)^{2/n}$ versus hv. Extrapolation of the line to the base line, where the value of $(Ahv)^{2/n}$ is zero, will give band gap energy.

Photoelectrochemical test (PEC)

The photoactivity of the samples were test in 0.01 M $[Fe(CN)_6]^{3-}/[Fe(CN)_6]^{4-}$ redox system by running linear sweep voltammetry technique (LSV) between two potentials limits (-1000 mV to 1000 mV versus Ag/AgCl). The BAS Potentiostat was used to control the process and to monitor the current and voltage profiles. The system consists of deposited film as a working electrode, platinum wire as counter electrode and Ag/AgCl as reference electrode. The photocurrent (I_p) and darkcurrent (I_d) of the PEC cells were recorded under light illumination and dark condition. The halogen lamp (300 W) was used for illuminating the electrode. The light path towards the PEC cells was chopped manually to study the effect on photoactivity behavior.

Energy dispersive and x-ray analysis (EDAX)

The elemental composition of the films was studied by scanning the electron microscope (JEOL JSM 6400) attached with energy dispersive analysis of the X-ray (EDAX) analyzer.

Chemical Bath Deposition of Thin Films

The influence of bath temperature and deposition time on films

The chemical bath deposition process is a slow process which facilitates better orientation of crystallites with improved grain structures. Here, the effect of deposition temperature (40°C to 60°C) towards the properties of thin films was investigated. The experiments were carried out for 80 min at 50°C in acidic medium (pH 1.5) using 0.05M of copper sulphate, tin chloride and sodium thiosulfate. The presence of 0.05M Na_2EDTA improves the lifetime of chemical bath as well as to improve quality of thin films.

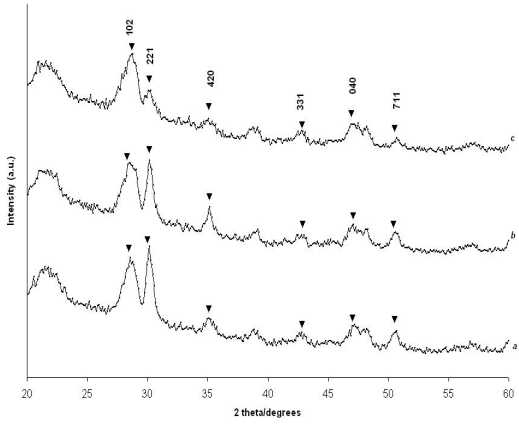

Figure 1: X-ray diffraction patterns of Cu_4SnS_4 films deposited at different chemical bath temperatures.
[(a) 40°C (b) 50°C (c) 60°C [Cu_4SnS_4 (▲)]

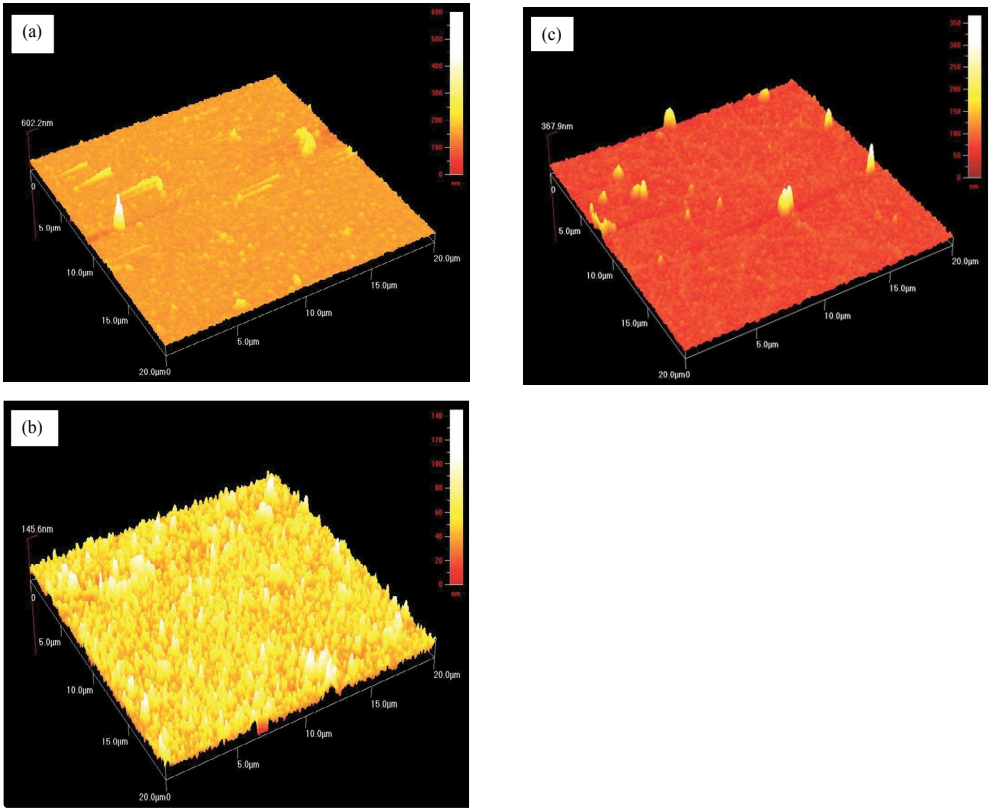

Figure 2: Atomic force microscopy images of Cu4SnS4 films deposited at different chemical bath temperatures [(a) 40°C (b) 50°C (c) 60°C]

X-Ray Diffraction (XRD) method is one of the most convenient tools for qualitative and quantitative analysis of crystalline compounds. The information obtained includes types and nature of crystalline phases as reported by many researchers [81-103]. X-rays are not absorbed very much by air, so the specimen need not be in an evacuated chamber. **Figure 1** shows the XRD patterns of the films deposited at different chemical bath temperatures. All the samples showed a polycrystalline in nature. There are six peaks occurred at 2θ =28.6°, 30.1°, 35.2°, 42.9°, 47.2° and 50.6° were detected for the films deposited at 40°C, 50°C and 60°C respectively. The corresponding *d*-spacing values are well in agreement with JCPDS data (Reference code: 010710129) of 3.12, 2.96, 2.54, 2.10, 1.92 and 1.80Å which attributed to the (102), (221), (420), (331), (040) and (711) planes, respectively. All these peaks are related to the compound of Cu_4SnS_4 of orthorhombic structure (a=13.5580Å, b=7.6810Å, c=6.4120Å, α=β=γ=90°). As the chemical bath temperature is increased from 40°C to 50°C, the intensity of diffraction peak (211) increases and this peak becomes narrower indicating an improvement of the crystallinity.

On the other hand, the thickness of the films was investigated using AFM images. At the right side of the images, an intensity strip is shown, which indicates the depth and height along the *z*-axis. The thickness values of 602, 146 and 368 nm have been observed for samples deposited at 40°C, 50°C and 60°C, respectively. This result indicates that bath temperature have great influence on the morphology of thin films.

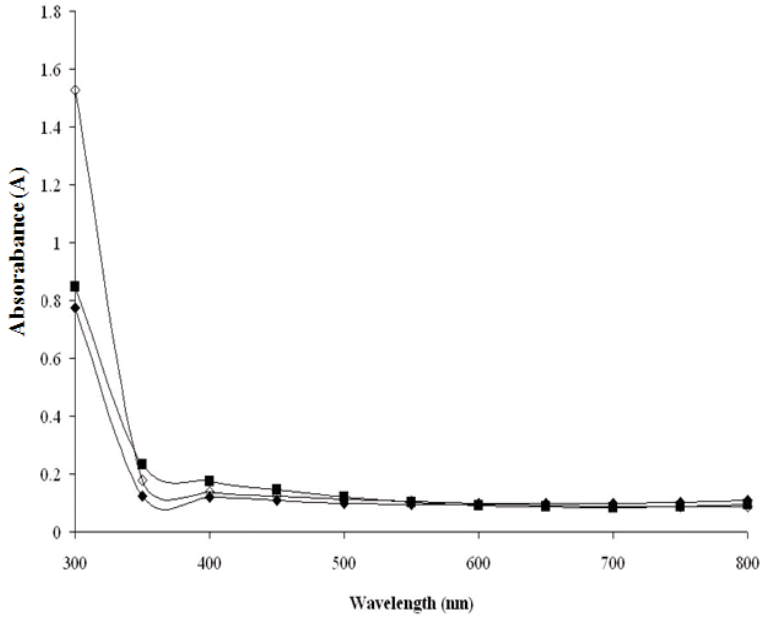

Figure 3: Optical absorbance versus wavelength of the Cu4SnS4 films deposited at different chemical bath temperatures (♦40°C; ◊ 50°C; ■ 60°C).

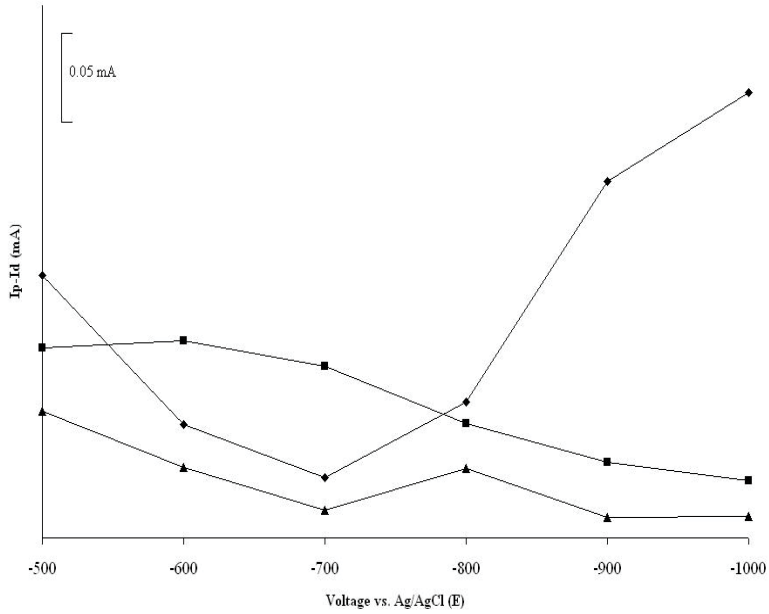

Figure 4: Comparison of photosensitivity of the films deposited at different chemical bath temperatures (♦50 °C; 40 °C; ■ 60 °C)

Based on the studies of the effect of deposition temperature, 50°C was found to be the optimum deposition temperature to produce good quality thin films under the current conditions. The thin films were deposited at different deposition periods (40-180 min)

in order to investigate the best conditions for the deposition process; other deposition parameters were maintained as before. (deposition temperature=50°C, pH 1.5, solutions concentration=0.05M, Concentration of Na_2EDTA=0.05M).

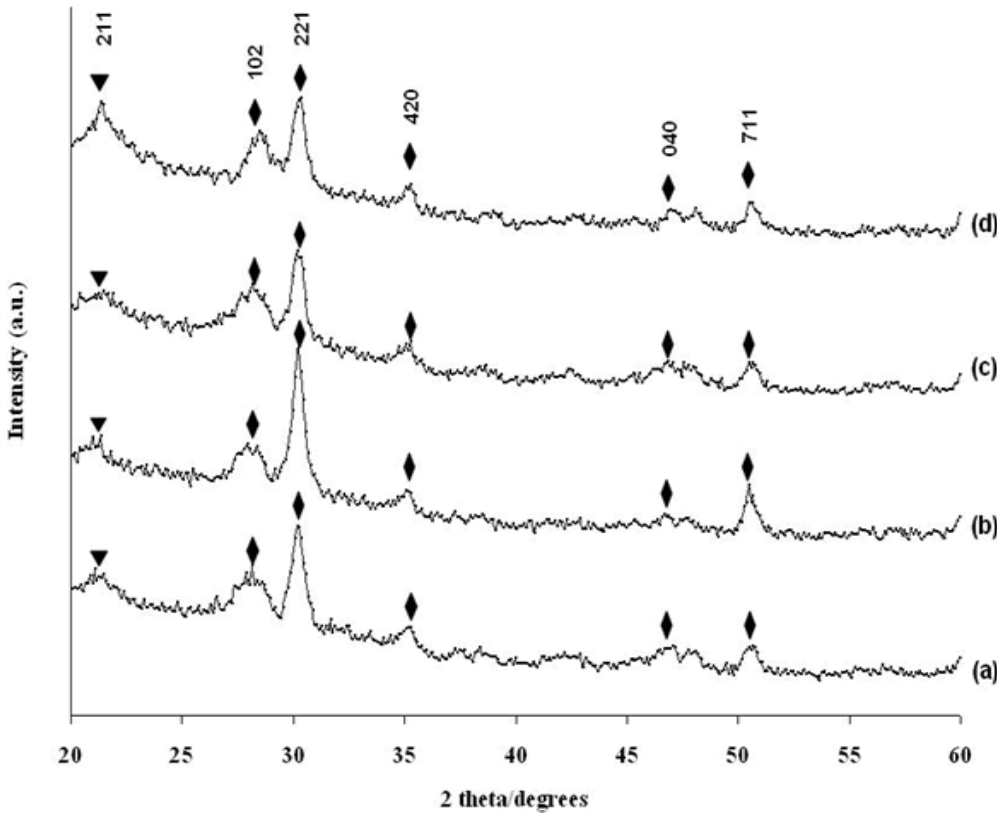

Figure 5: X-ray diffraction patterns of Cu4SnS4 thin films deposited at different deposition periods (a) 40 min (b) 80 min (c) 150 min (d) 180 min [Cu4SnS4•, indium tin oxide▼].

Figure 5 shows the X-ray diffraction (XRD) patterns of Cu4SnS4 thin films deposited at different deposition periods. The XRD patterns from all the samples have shown a major diffraction peak at 2θ=30.2° which is corresponding to (221) orientation of orthorhombic structure of Cu4SnS4. In addition to the (221) plane, we also observed other diffraction peaks at 2θ = 28.5°, 35.2°, 47.2° and 50.6° which are attributed to (102), (420), (040) and (711) planes, respectively.

In particular, the film deposited for 80 min showed higher intensity for all diffraction peaks indicating that this deposition period is favorable for the Cu_4SnS_4 films growth. The observed *d*-spacing values were compared with standard *d*-spacing values (Reference code: 01-071-0129) and are in good agreement with standard *d*-spacing values. On the other hand, the presence of the indium tin oxide peaks (Reference code: 01-089-4598) in the XRD patterns is due to the glass substrate used during deposition. There is only single peak occurred at 2θ = 21.3° corresponding to (211) plane was detected as shown in **Figure 5 (a)-(d)**. According to XRD patterns, the higher intensity of Cu_4SnS_4 peaks could be observed as compared to the substrate peaks.

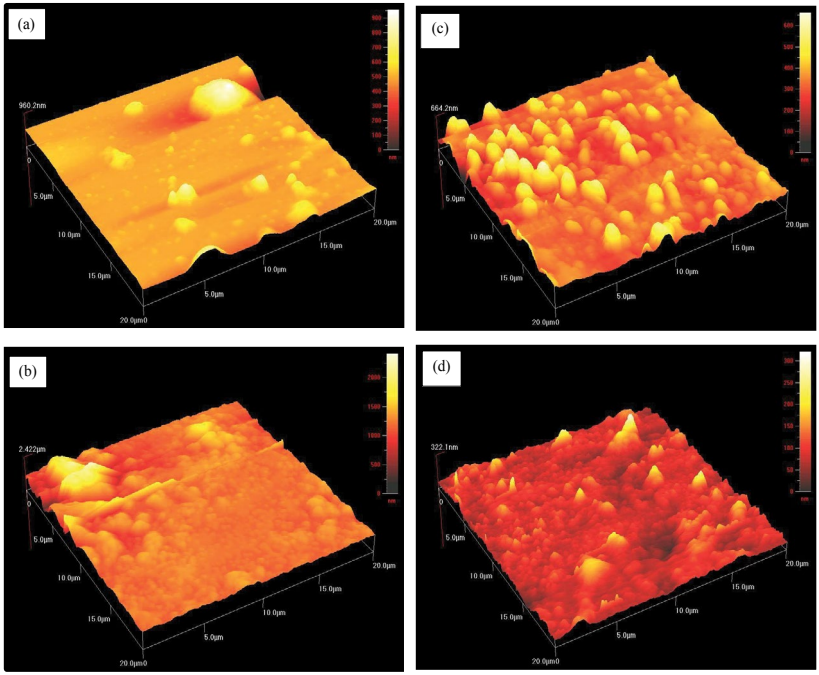

Figure 6: Atomic force microscopy images of Cu_4SnS_4 thin films deposited at different deposition periods (a) 40 min (b) 80 min (c) 150 min (d) 180 min.

Figure 6 shows three-dimensional AFM images (20 μm X 20 μm) for Cu_4SnS_4 thin films deposited onto ITO glass substrates at different deposition periods. The films deposited at 40 min showed incomplete coverage of material over the surface of substrates (**Figure 6a**). It is also pointed out that the film formation was irregular and the film thickness was estimated to be 960 nm. As the deposition time was increased to 80 min, more surface coverage was noticed. There are more materials to be deposited onto substrate and thicker film (2422 nm) to be formed (**Figure 6b**). However, thinner films could be observed when the deposition time was increased further to 150 min (664 nm) and 180 min (322 nm), respectively as shown in **Figure 6c and 6d**.

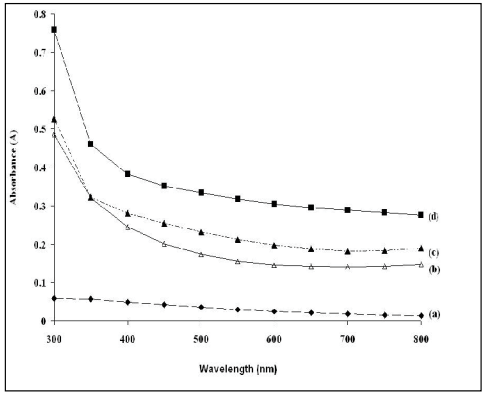

Figure 7: Optical absorbance versus wavelength of the Cu_4SnS_4 thin films deposited at different deposition periods (a) 80 min (b) 150 min (c) 180 min (d) 80 min

The optical properties of Cu_4SnS_4 thin films were measured in the range of 300-800 nm using UV-Vis Spectrophotometer. **Figure 7** presents the absorbance spectra of Cu_4SnS_4 thin films deposited at different deposition periods. The results showed that the film deposited at 80 min produced higher absorption characteristics as compared with other deposition periods. This could be due to thicker films formed onto surface of the substrate.

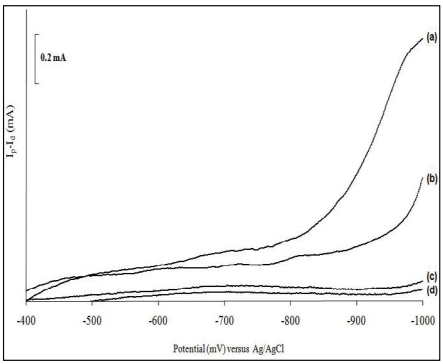

Figure 8: Difference between photocurrent and dark current for the Cu_4SnS_4 thin films deposited at various deposition periods (a) 80 min (b) 150 min (c) 180 min (d) 40 min.

Figure 8 shows the difference between photocurrent (Ip) and dark current (Id) response for the Cu4SnS4 thin films deposited at various deposition periods in contact with [Fe(CN)6]3-/[Fe(CN)6]4- redox system solution. When the deposition time was increased from 40 to 80 min, the difference in the photoresponse increased. This is due to more Cu4SnS4 grains are exposed towards the redox system. The results are match with AFM analysis. The decrease in the difference between the photocurrent and dark current could be observed as the deposition time was increased to 180 min. The current change with illumination exhibits semiconductor behavior of the materials. Apparently, the photocurrent occurs on negative potential shows the films prepared are of p-type material.

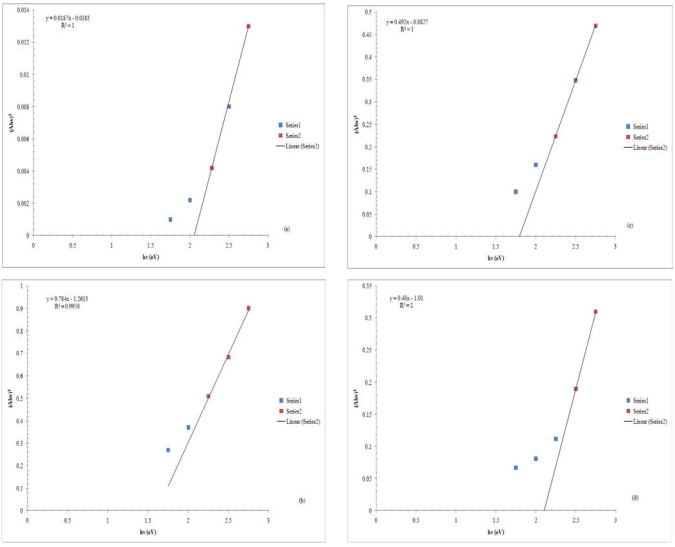

Figure 9: Plot of $(Ahv)^{2/n}$ versus hv when n=1 of the Cu_4SnS_4 thin films deposited at different deposition periods. (a) 40 min (b) 80 min (c) 150 min (d) 180 min

Band gap energy and transition type can be derived from mathematical treatment of data obtained from optical absorbance versus wavelength with Stern relationship of near-edge absorption.

$$A = \frac{[k\left(h\upsilon - E_g\right)^{n/2}]}{h\upsilon}$$

Where υ is the frequency, h is the Planck's constant, k equals a constant while n carries the value of either 1 or 4. The value of n is 1 and 4 for the direct transition and indirect transition, respectively. **Figure 9** shows the plot of $(A h\upsilon)^2$ versus $h\upsilon$ for Cu_4SnS_4 thin films deposited under various pH values. The band gap values were determined from the intercept of the straight-line portion of the $(A h\upsilon)^2$ against the $h\upsilon$ graph on the $h\upsilon$-axis using computer fitting program. The linear part shows that the mode of transition in these films is of direct nature. The band gaps deduced for all thin films in this manner decreased from 2.1 eV to 1.6 eV as the deposition time was increased from 40 to 80 min. However, the band gap was found slightly increased to 1.8 and 2.1 when the deposition time was further increased to 150 and 180 min, respectively.

The influence of solution concentration and complexing agent on films

Based on the studies of the effect of deposition time, 80 min was found to be the best deposition time to produce good quality thin films under the current conditions. In order to study the effect of electrolytes concentration on the film properties, deposition at various concentrations was carried out. The first set of experiment was carried out using constant concentration of 0.05M of $CuSO_4$, $SnCl_2$ and varying concentrations of $Na_2S_2O_3$ (0.01M and 0.05M) solutions.

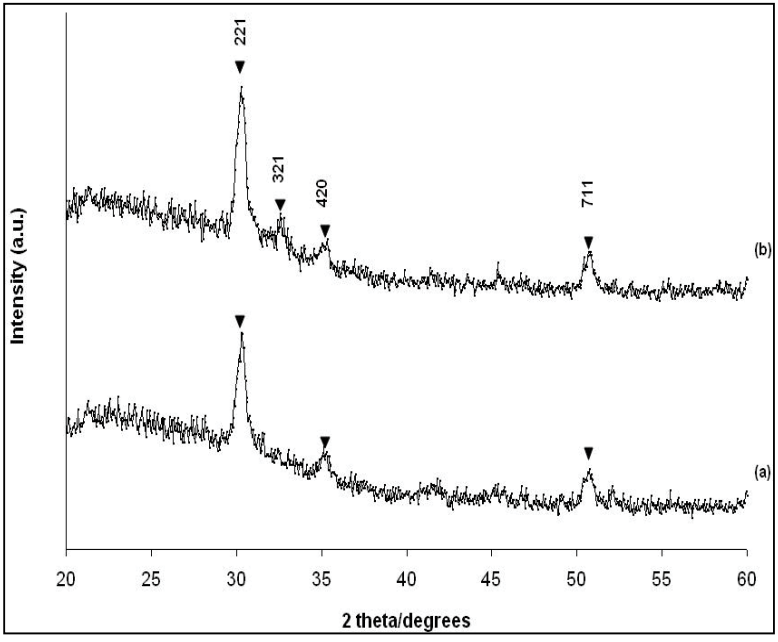

Figure 10: XRD patterns of samples prepared at various $CuSO_4$ concentrations:(a) 0.01M (b) 0.05M. Concentration of $SnCl_2$ and $Na_2S_2O_3$ are fixed at 0.05M. [Cu_4SnS_4 (▲)]

The second set of experiment was carried out using fixed concentration of 0.05M of CuSO4, Na2S2O3 and varying concentrations of SnCl2 (0.01M and 0.05M) solutions.

The third set of experiment was carried out using constant concentration of 0.05 M of SnCl2, Na2S2O3 and varying concentrations of CuSO4 (0.01M and 0.05M) solutions. Other deposition parameters were maintained as before. (deposition temperature=50°C, pH 1.5, deposition time=80 min, concentration of Na2EDTA=0.05M).

Figure 10 shows the XRD patterns of the films deposited at various CuSO4 concentrations (0.01 and 0.05M) and constant Na2S2O3, SnCl2 at 0.05M. The film prepared using 0.01M CuSO4 showed three peaks at 2θ =30.1, 35.3° and 50.5° corresponding to interplanar distances of 2.96, 2.54 and 1.80Å respectively. These peaks are in a good agreement with the JCPDS data (Reference code: 010710129) for Cu4SnS4 (a =13.5580Å, b = 7.6810Å, c = 6.4120Å, α = β = γ =90°). As the concentration of CuSO4 was increased to 0.05 M, the intensity of peak corresponding to (221) plane increased. Also, the additional peak corresponding to 2.67Å at 2θ =33.2° was obtained.

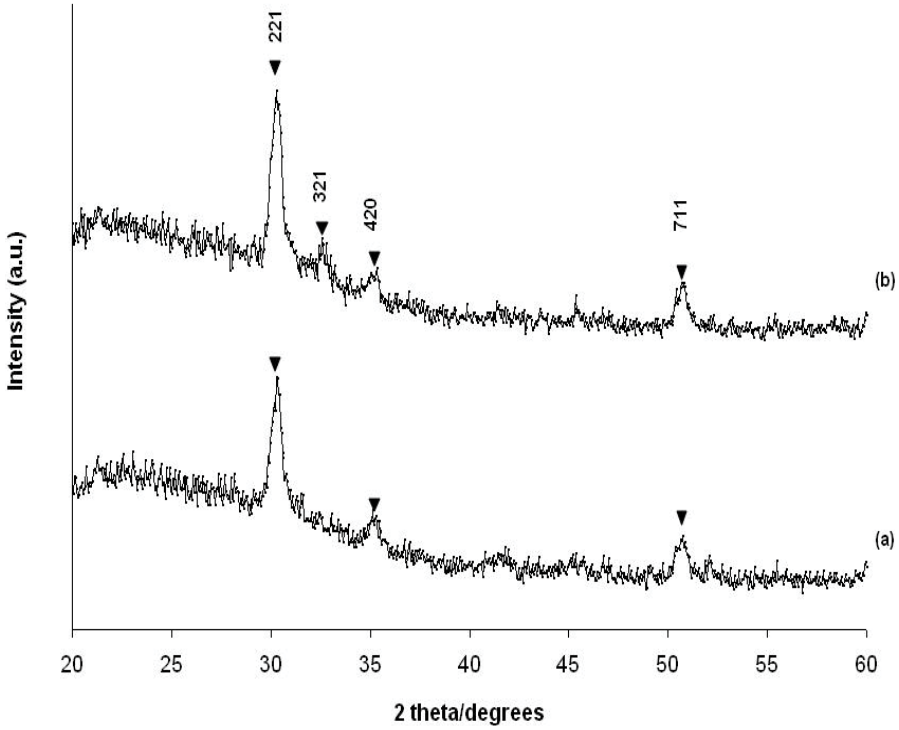

Figure 11: XRD patterns of samples prepared at various $SnCl_2$ concentrations: (a) 0.01M (b) 0.05M. Concentration of $CuSO_4$ and $Na_2S_2O_3$ are fixed at 0.05 M. [Cu_4SnS_4 (▲)]

Figure 11 shows the XRD patterns of the films deposited at various SnCl2 concentrations (0.01M and 0.05M) and fixed Na2S2O3, CuSO4 at 0.05M. Each pattern contains several diffraction peaks indicating that the films are polycrystalline in nature. There are three Cu4SnS4 peaks at 2θ =30.1°, 35.1° and 50.5° for the sample prepared at lower concentration of SnCl2 (0.01M). The corresponding interplanar distances are well in agreement with the JCPDS data of 2.96, 2.55 and 1.80Å. When the concentration of SnCl2 was increased to 0.05 M, the intensity of (221) plane increased. This is accompanied by the appearance of two other peaks of Cu4SnS4 at 2θ =28.6° and 46.4° with interplanar distances of 3.14 and 1.95Å.

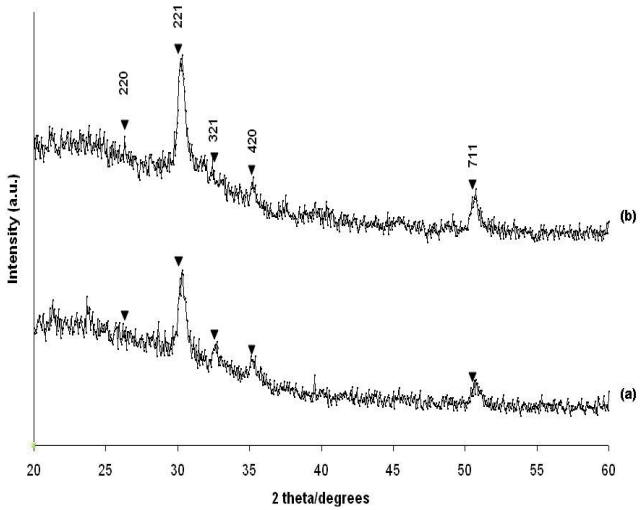

Figure 12: XRD patterns of samples prepared at various $Na_2S_2O_3$ concentrations: (a) 0.01 M (b) 0.05 M. Concentration of $CuSO_4$ and $SnCl_2$ are fixed at 0.05M. [Cu_4SnS_4 (▲)]

Figure 12 shows the XRD patterns of the films deposited at various Na2S2O3 concentrations (0.01M and 0.05M) with constant CuSO4, SnCl2 at 0.05M. There are five Cu4SnS4 peaks at 2θ =26.5°, 30.1°, 33.1°, 35.1° and 50.7°, corresponding to d-spacing values 3.36 2.96, 2.68, 2.55 and 1.79Å for the samples prepared at 0.01M and 0.05M of Na2S2O3. Comparison between the films deposited at 0.01M and 0.05M of Na2S2O3 showed that the intensity of the peaks increased indicating greater crystallinity as the concentration was increased. This could be seen in the (221) plane which is more intense.

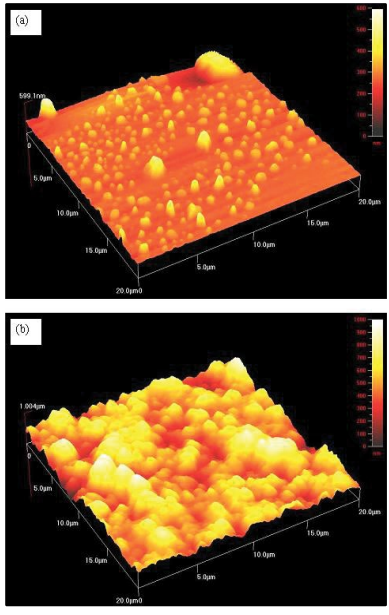

Figure 13: Atomic force microscopy images of Cu_4SnS_4 films deposited at various $CuSO_4$ concentrations: (a) 0.01M (b) 0.05M. Concentration of $Na_2S_2O_3$ and $SnCl_2$ are fixed at 0.05M

Figure 13 shows the AFM images of films prepared at different CuSO4 concentrations (0.01M and 0.05M) and constant SnCl2, Na2S2O3 at 0.05M. The film prepared using 0.01M CuSO4 showed low appearance of grains over the substrate. The size of the grains varies from one another and randomly distributed over ITO substrate.

However, the film prepared using 0.05M CuSO4 indicated better morphology compared to the lower concentration. The grain size of these films was much bigger and has complete coverage over the substrate surface. This result is consistent with the observation from XRD. On the other hand, the film thickness was investigated using atomic force microscopy images. We can conclude that the films deposited using lower solution concentration (0.01M) have thinner surface (599.1 nm) while the films deposited at higher solution concentration (0.05M) produce thicker films (1004 nm).

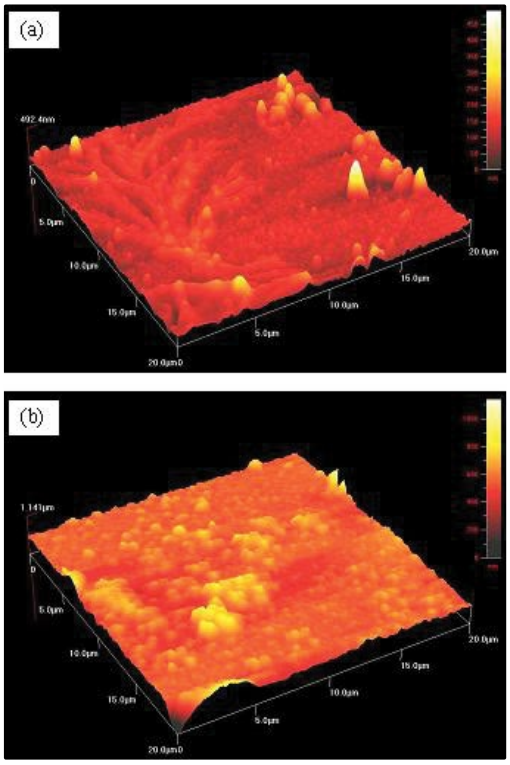

Figure 14: Atomic force microscopy images of Cu_4SnS_4 films deposited at various $SnCl_2$ concentrations: (a) 0.01M (b) 0.05M. Concentration of $Na_2S_2O_3$ and $CuSO_4$ are fixed at 0.05M

Figure 14 shows the AFM images of films prepared at different SnCl2 concentrations (0.01M and 0.05M) and constant Na2S2O3, CuSO4 at 0.05M. The AFM image of film prepared using 0.01M SnCl2 showed the surface of substrate was not covered completely. This observation suggests an incomplete nucleation step with irregular growth rate of the grains. However, there seems increase in the number of grains for the film deposited at 0.05M SnCl2. The surface of the ITO glass substrate was covered completely as can be seen in Figure 14a and b. On the other hand, the film thickness was investigated using atomic force microscopy images. We can conclude that the films deposited using lower solution concentration (0.01M) have thinner surface (492.4 nm) while the films deposited at higher solution concentration (0.05M) produce thicker films (1142 nm).

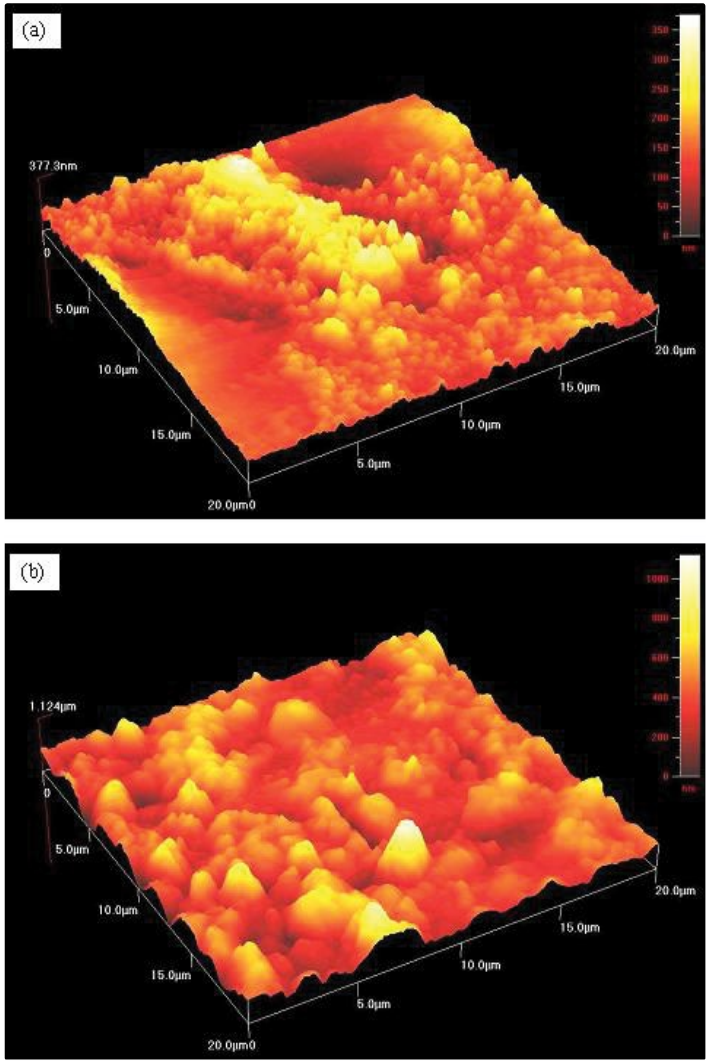

Figure 15: Atomic force microscopy images of Cu_4SnS_4 films deposited at various $Na_2S_2O_3$ concentrations:(a) 0.01M (b) 0.05M. Concentration of $SnCl_2$ and $CuSO_4$ are fixed at 0.05M

Figure 15 shows the AFM images of films prepared at different Na2S2O3 concentrations (0.01M and 0.05M) and constant SnCl2, CuSO4 at 0.05M. The images pointed out that the deposits are crystalline and their grain size varies with the variation of Na2S2O3 concentrations. The sample prepared at 0.01M of Na2S2O3 exhibits smaller crystal size (Figure 15a) while sample prepared at 0.05M of Na2S2O3 leads to bigger crystal size (Figure 15b). The sample prepared at higher concentration showed the surface of the substrate was covered completely. The size of the grains varied from 1 to 2 µm. The improvement of crystallinity of the film is consistent with the results of XRD. On the other hand, the film thickness was investigated using atomic force microscopy images. We can conclude that the films deposited using lower solution concentration (0.01M) have thinner surface (377.3 nm) while the films deposited at higher solution concentration (0.05M) produce thicker films (1124 nm).

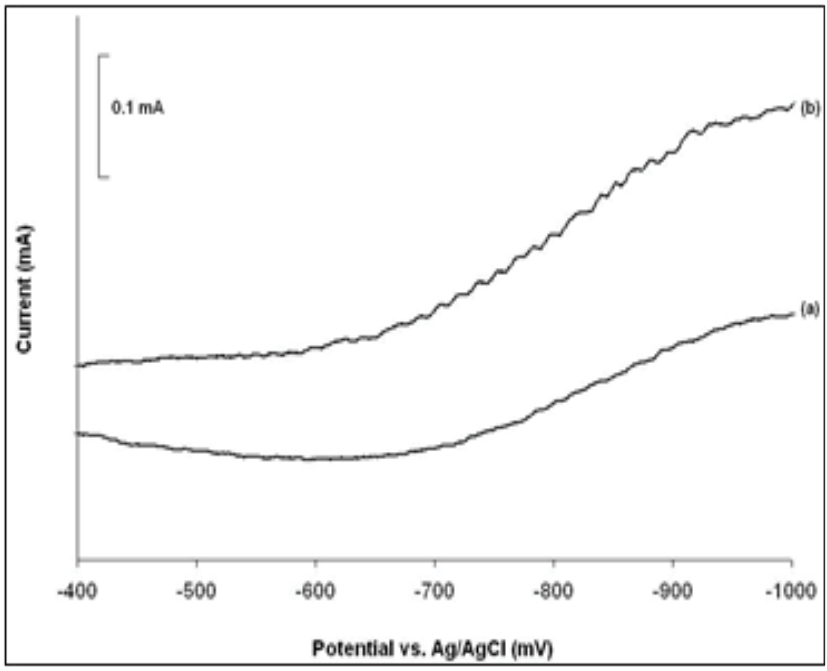

Figure 16: The photoresponse of the Cu_4SnS_4 films deposited at various $CuSO_4$ concentrations: (a) 0.01M and (b) 0.05M. Concentration of $SnCl_2$ and $Na_2S_2O_3$ are fixed at 0.05M

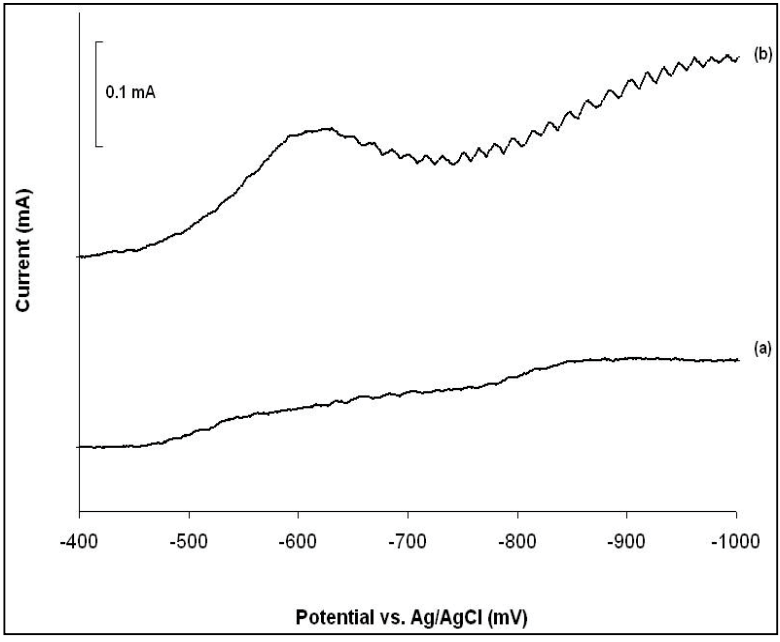

Figure 17: The photoresponse of the Cu_4SnS_4 films deposited at various $SnCl_2$ concentrations: (a) 0.01M and (b) 0.05M. Concentration of $CuSO_4$ and $Na_2S_2O_3$ are fixed at 0.05M

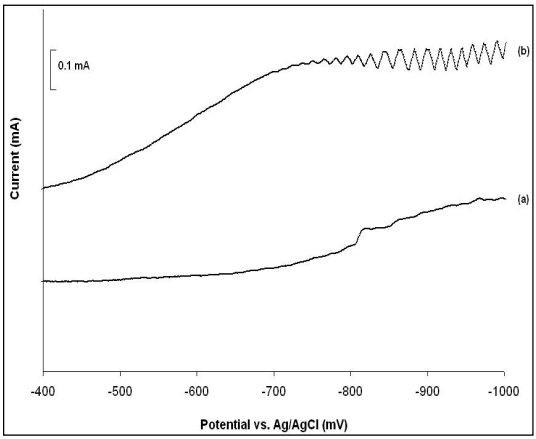

Figure 18: The photoresponse of the Cu_4SnS_4 films deposited at various $Na_2S_2O_3$ concentrations (a) 0.01M and (b) 0.05M. Concentration of $SnCl_2$ and $CuSO_4$ are fixed at 0.05M

Figure 16, Figure 17 and Figure 18 show the photoresponse of the films prepared using different concentrations of CuSO4, SnCl2 and Na2S2O3, respectively. The current change with the illumination confirms that the films possess semiconducting behavior. The films prepared using higher concentration (Figure 16b-18b) showed better photosensitivity compared with lower concentration (Figure 16a-18a). This is probably due to the improved crystal compactness or density of the deposit. The fact that the photocurrent occurs on the negative potential indicates the films prepared are p-type semiconductor.

The use of complexing agents is very common in the preparation of thin films through the chemical bath deposition method [104-133]. In this study, the disodium ethylenediaminetetraacetic acid (Na2EDTA) is used as complexing agent to improve the lifetime of chemical bath as well as the quality of thin films. In order to investigate the influence of the complexing agents on the chemical bath deposited films, the deposition was carried out under different concentrations of Na2EDTA ranging from 0.01M to 0.10M. Other experimental set-up was maintained as mentioned before. (deposition temperature=50°C, pH 1.5, solutions concentration=0.05M, deposition time=80 min).

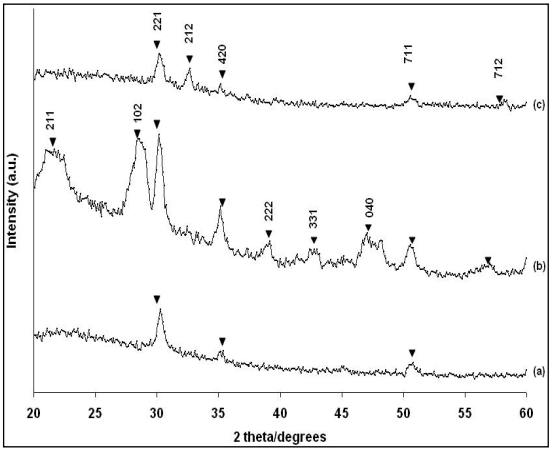

Figure 19: X-ray diffraction patterns of the Cu_4SnS_4 thin films deposited at different concentrations of Na_2EDTA. (a) 0.01 M(b) 0.05M (c) 0.10M

Figure 19 shows the XRD patterns of the films deposited at different concentrations of Na2EDTA. All the samples showed a polycrystalline in nature. There are nine peaks occurred at 2θ =22.3°, 28.4°, 30.2°, 35.1°, 39.1°, 42.8°, 47.0°, 50.6° and 56.6° were detected for the films deposited with 0.05 M Na2EDTA (Figure 19b). The XRD data obtained matches the standard JCPDS data (Reference code: 010710129) for orthorhombic phase of Cu4SnS4. (a =13.5580Å, b = 7.6810Å, c = 6.4120Å,

α = β = γ =90°). However, the number of Cu4SnS4 peaks decreased to three (Figure 19a) and five (Figure 19c) for the films deposited with 0.01M and 0.10M Na2EDTA, respectively. The strongest peak for all samples occurred at 2θ =30.2° with d-spacing value of 2.96Å. This indicates that the preferred orientation lies along (221) direction for the chemical bath deposited Cu4SnS4 thin film. The (221) plane showed the highest intensity peak for the film deposited using 0.05M Na2EDTA indicating more favorable condition for the formation of thin film.

The AFM measurements were performed to study the differences in the surface morphology for the samples deposited under different concentrations of Na2EDTA. Figure 20 shows the AFM images of thin film deposited with 0.01M, 0.05M and 0.10M Na2EDTA on a scale of 20 µm x 20 µm. Comparing the three AFM images, it is clearly seen that the surface of the film deposited with 0.05M Na2EDTA is very smooth. The material was found to cover the surface of the substrate completely.

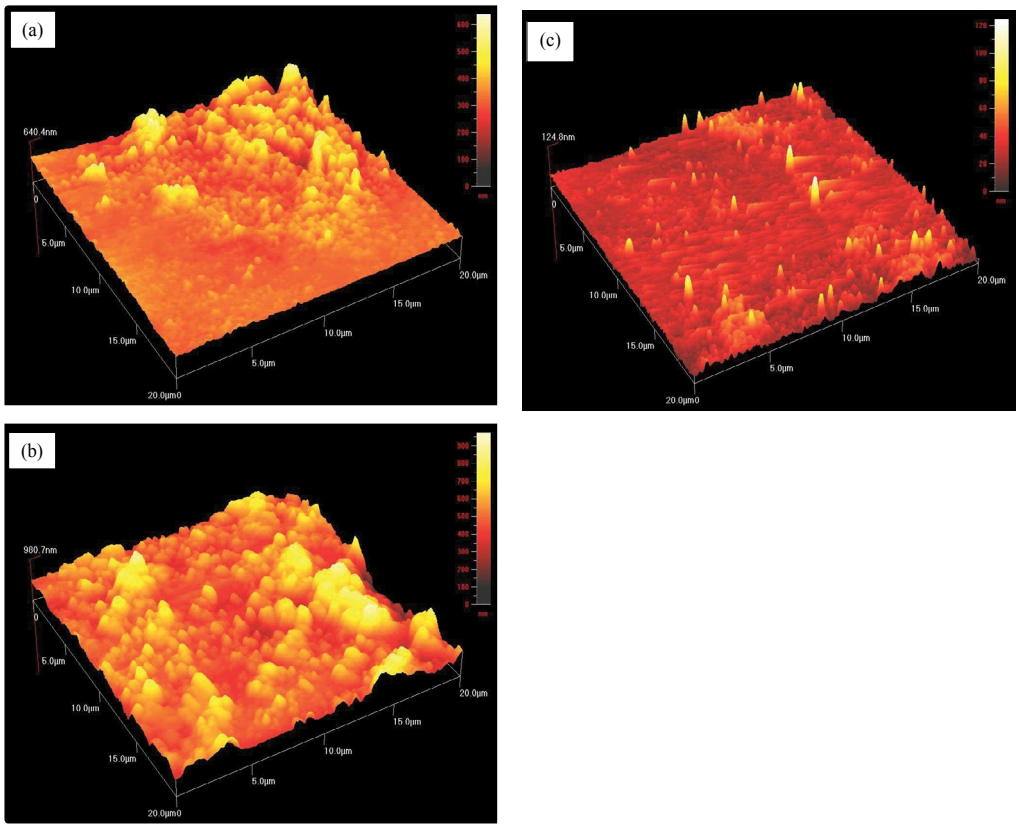

Figure 20: The atomic force microscopy images of the Cu_4SnS_4 thin films deposited at different concentrations of Na_2EDTA. (a) 0.01M (b) 0.05M (c) 0.1M

Formation of grain was uniformly distributed over the deposit layer could be observed (Figure 20b). The sizes of these grains are quite similar and vary from 0.9 to 1.2 μm. The morphology study shows that the thin films obtained with 0.01M and 0.10M Na2EDTA are very thin, not compact and incomplete coverage over the substrate surface (Figure 20a and 20c). On the other hand, the thickness of thin film was increased from 640 nm to 981 nm as the concentration of Na2EDTA was increased from 0.01M to 0.05M. However, the thickness of the thin films was reduced (125 nm) as the concentration of Na2EDTA was further increased to 0.1M. Based on the AFM results, we can conclude that the presence of Na2EDTA has great influence on the properties of thin films.

Optical properties of thin films have been investigated by many researchers using UV-Visible spectrophotometer. The absorption spectra and band gap value will be reported as shown in their paper [134-150].

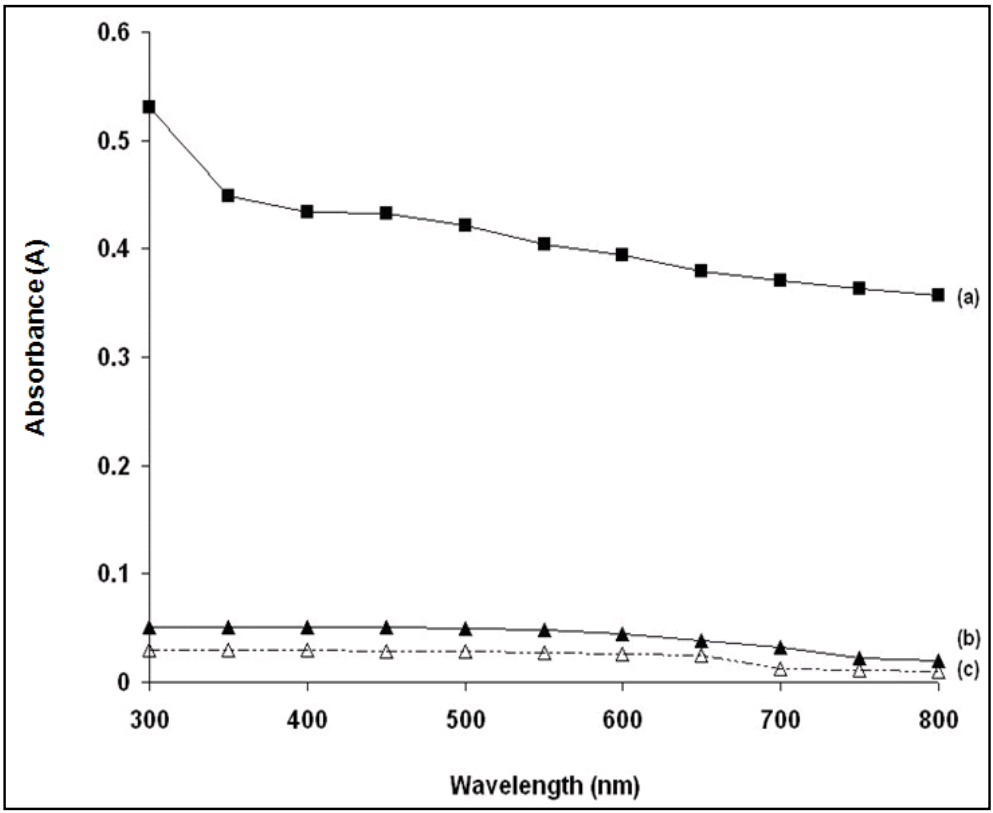

Figure 21: The optical absorption versus wavelength of the Cu_4SnS_4 thin films deposited at different concentrations of Na_2EDTA. (a) 0.05M (b) 0.10M (c) 0.01M.

The optical properties of thin films were measured in the range of 300-800 nm by using UV-Vis spectrophotometer. Figure 21 shows the absorption spectra of the samples deposited with different concentrations of Na2EDTA, ranging from 0.01M to 0.10M. With increasing concentration of Na2EDTA from 0.01M to 0.05M, the absorption value of the films increases (Figure 21c and 21a) and then decreases at higher Na2EDTA concentration (Figure 21b). It is believed that the complexing reaction was complete with higher concentration of complexing agent. Therefore, hinders the deposition of Cu4SnS4 thin films.

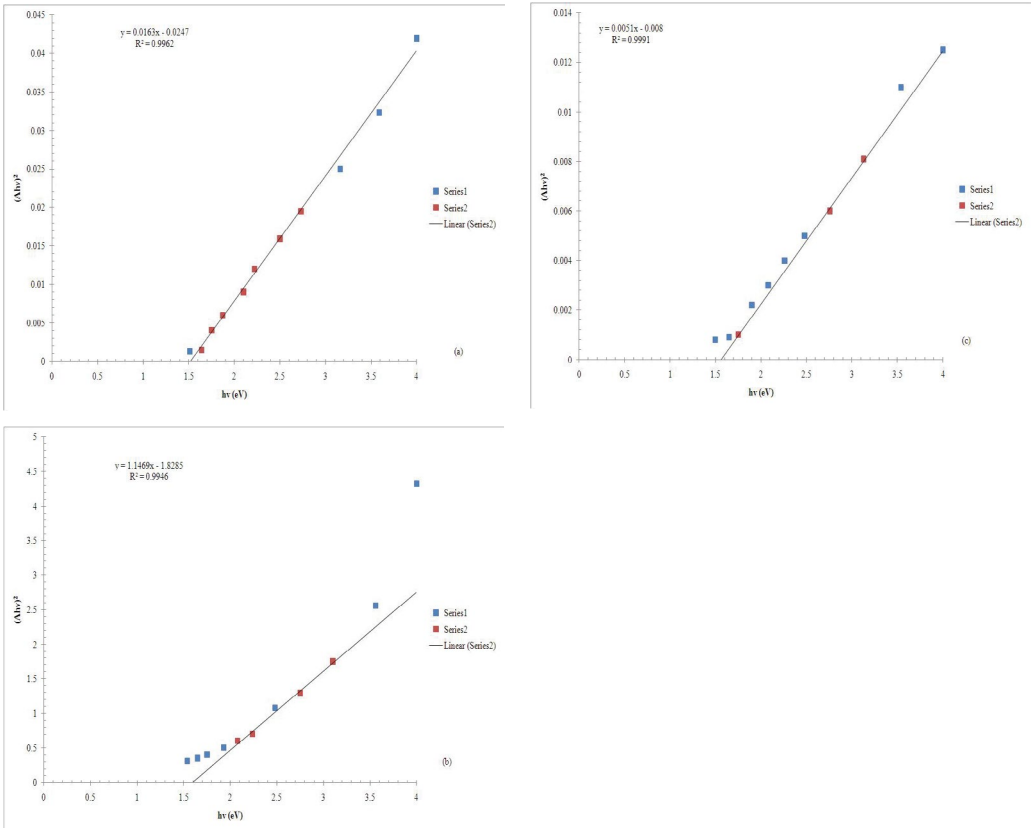

Figure 22: Plot of $(Ahv)^{2/n}$ versus hv when n=1 of the Cu_4SnS_4 thin films deposited at different concentrations of Na_2EDTA. (a) 0.01M (b) 0.05M (c) 0.1M

Figure 22 shows the plot of (Ahv)2 versus hv for Cu4SnS4 thin films deposited under various pH values. The band gap values were determined from the intercept of the straight-line portion of the (Ahv)2 against the hv graph on the hv-axis using computer fitting program. The linear part shows that the mode of transition in these films is of direct nature. The band gaps deduced for all thin films in this manner increased from 1.56 eV to 1.60 eV as the concentration of Na2EDTA was increased from 0.01M to 0.05M. However, the band gap was found slightly reduced to 1.59 when the concentration of Na2EDTA was further increased to 0.1M

The influence of various pH values on films

From the data obtained, we can conclude that the optimum concentration of Na2EDTA is 0.05M. The following experiment was carried out using this Na2EDTA concentration to study the optimum pH value. Other experimental conditions were not altered to maintain a constant approach towards uniform set-up. (deposition temperature = 50°C, deposition time = 80 min, solutions concentration = 0.05M, concentration of Na2EDTA = 0.05M).

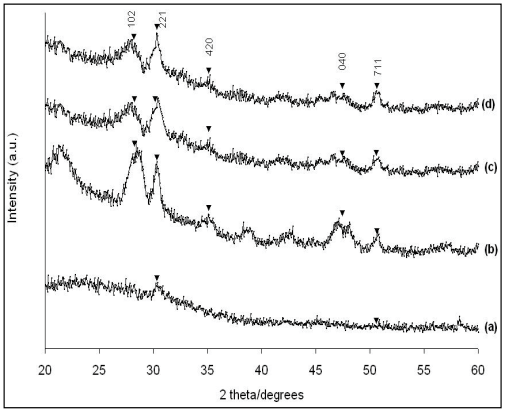

Figure 23: X-ray diffraction patterns of Cu_4SnS_4 thin films chemically deposited for 80 min at different pH (a) pH 0.5 (b) pH 1.0 (c) pH 1.5 (d) pH 2.0 [Cu_4SnS_4 ▲]

Figure 23 shows the XRD patterns of thin films chemically deposited for 80 min at different pH ranging from 0.5 to 2. The chemical bath deposited thin films are found to be polycrystalline in nature. The films prepared at pH 0.5 produced two peaks at 2θ = 30.3º and 50.6º corresponding to d-spacing values of 2.95 and 1.81Å, respectively. The observed d-spacing values were compared with standard d-spacing values (Reference code: 010710129) and are in good agreement with standard d-spacing values. As the pH value was increased to 1.5, the intensity of the peak corresponding to (221) plane increased. This is accompanied by the appearance of three other peaks which attribute to Cu4SnS4 at 2θ = 28.6º, 35.5º and 47.1º with d-spacing values of 3.12, 2.56 and 1.91Å for the films deposited at pH 1.0, 1.5 and 2.0 respectively.

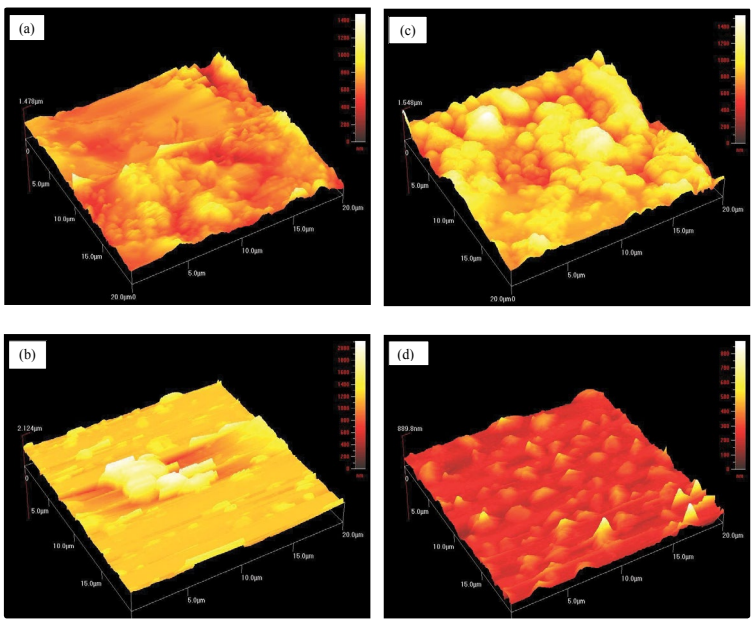

Figure 24: Atomic force microscopy images of Cu_4SnS_4 thin films chemically deposited for 80 min at different pH. (a) pH 0.5 (b) pH 1.0 (c) pH 1.5 (d) pH 2.0

Figure 24 shows three-dimensional AFM images for an area of 20 μm X 20 μm for Cu4SnS4 thin films. These films were chemically deposited for 80 min at different pH ranging from 0.5 to 2. The irregular surface of films is detected for the sample deposited at pH 0.5 (Figure 24a). Its three-dimensional image shows that larger surface roughness is observed. The discontinuous distribution of grains on the surface of substrate could be observed for the sample prepared at pH 1 (Figure 24b). When the pH was further increased to 1.5, the film shows uniform, dense and well-covered entire substrate surface (Figure 24c). However, the decreased of grain size could be observed as the pH was increased to 2 (Figure 24d).

On the other hand, the thickness of the films was studied using AFM images. At the right side of the images, an intensity strip is shown, which indicates the depth and height along the z-axis. The thickness values of 1478, 2124, 1548 and 890 nm have been observed for samples deposited at pH 0.5, 1.0, 1.5 and 2.0, respectively. This result indicates that an increase in pH up to 1 allows more materials to be deposited onto indium tin oxide substrate and thicker films to be formed. However, further increase in pH caused thinner films to be produced.

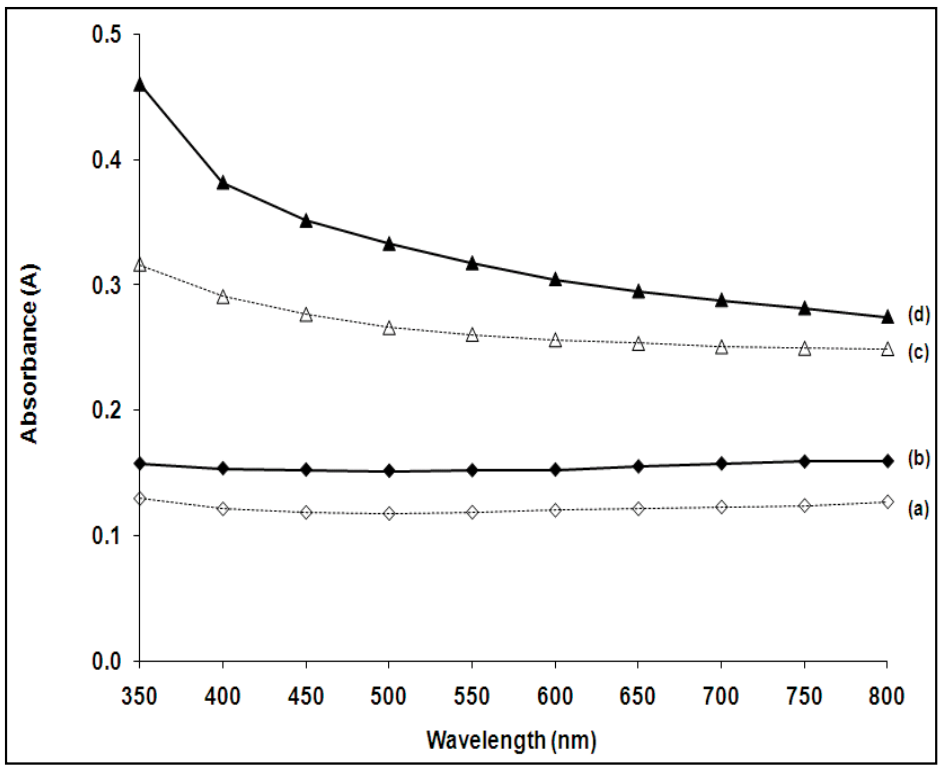

Figure 25: Optical absorbance versus wavelength of the Cu_4SnS_4 thin films chemically deposited for 80 min at different pH. (a) pH 0.5 (b) pH 1.0 (c) pH 2.0 (d) pH 1.5

Figure 25 shows the UV-Visible absorption spectra of the films grown from a chemical bath for 80 min under different pH values. The results show that the films deposited at pH 1.5 produced higher absorption characteristics as compared with other pH values. This response associated with the fact that more polycrystalline Cu4SnS4 materials are formed at this pH value. Thus, pH 1.5 is more preferable in the preparation of Cu4SnS4 films of better quality on ITO substrate.

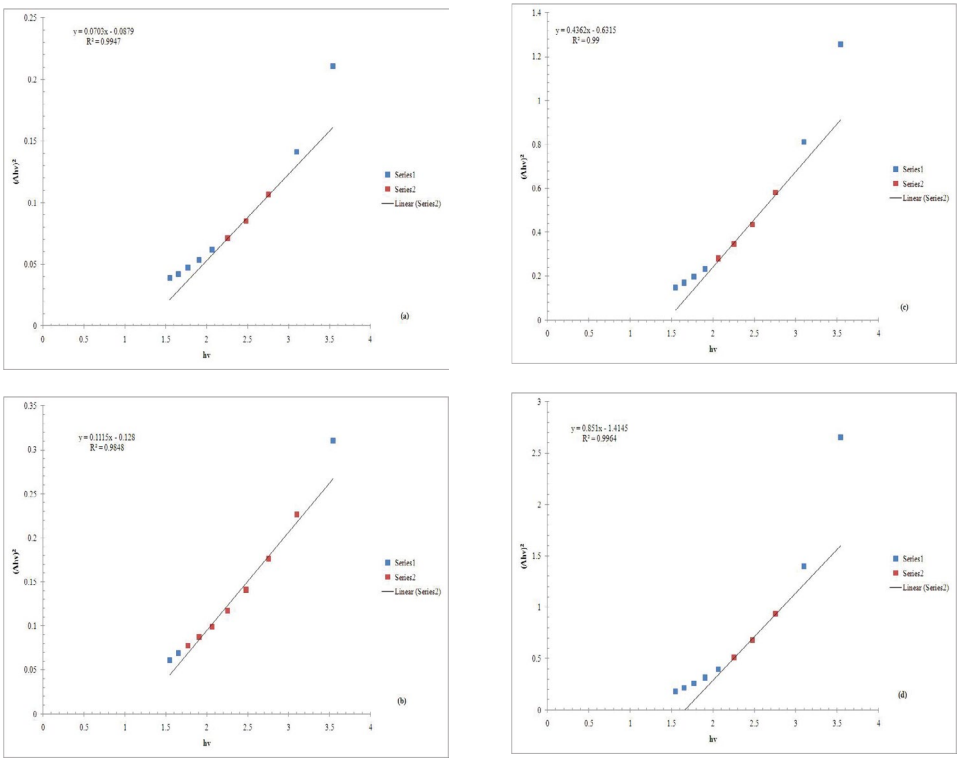

Figure 26: Plot of $(Ahv)^{2/n}$ versus hv when n=1 of the Cu_4SnS_4 thin films deposited at different pH values. (a) pH 0.5 (b) pH 1.0 (c) pH 1.5 (d) pH 2.0.

Band gap could be measured by using spectra using UV-Spectrophotometer. Figure 26 shows the plot of (Ahv)2 versus hv for Cu4SnS4 thin films deposited under various pH values. The band gap values were determined from the intercept of the straight-line portion of the (Ahv)2 against the hv graph on the hv-axis using computer fitting program. The linear part shows that the mode of transition in these films is of direct nature. The band gaps deduced for all thin films in this manner reduced from 1.24 eV to 1.17 eV as pH was increased from pH 0.5 to 1.0. However, the band gap was found increased to 1.45 and 1.62 eV, respectively when the pH was further increased to pH 1.5 and 2.

Finally, the different deposition parameters such as bath temperature (50°C), deposition time (80 min), Na2EDTA concentration (0.05M), solutions concentration (0.05M) and pH (pH 1.5) are optimized to obtain good quality of thin films. The compositional analysis of the thin films is carried out by the Energy Dispersive Analysis Of X-Ray (EDAX) technique. This tool is fast and easy to study chemical characterization of samples such as thin films and semiconductor [151-200]. The EDAX spectrum of the Cu4SnS4 thin films deposited under optimized deposition conditions is shown in Figure 27. The quantitative elemental analysis was carried out only for Cu, Sn and S. The atomic percentage (%) for these elements is 49.1, 12.6 and 38.3%, respectively. The ratio of 4:1:3 of copper (Cu), tin (Sn) and sulphur (S) has been confirmed by EDAX analysis. The sulphur concentration is slightly less as compared to stoichiometric of Cu4SnS4.

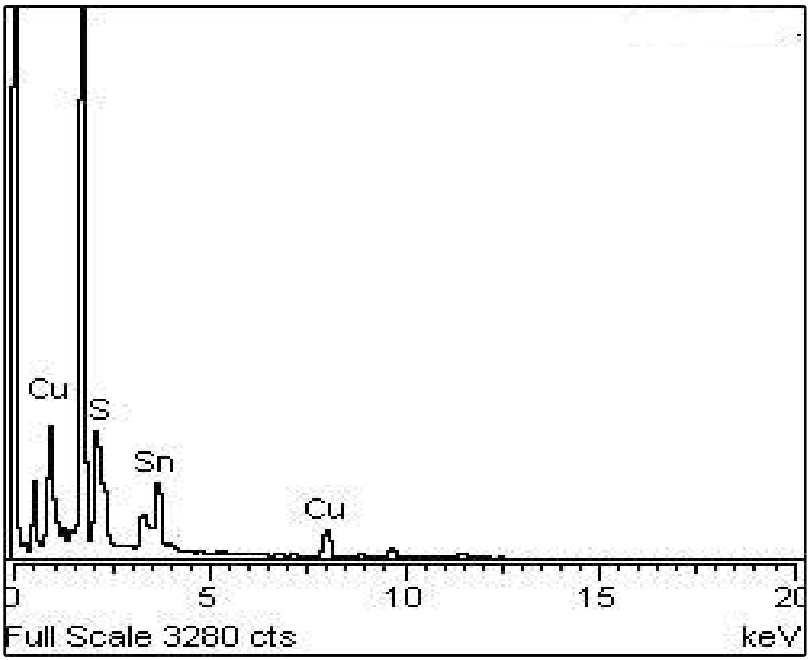

Figure 27: EDAX spectrum of Cu_4SnS_4 thin films deposited on indium tin oxide glass substrate at optimized parameters

References

1. Chet S, Matthew GP, Vahid A, Brian G., Bonil K, et al. (2009) Synthesis of Cu_2ZnSnS_4 nanocrystals for use in low cost photovoltaics. J Am Chem Soc 131: 12554-12555.
2. Ennaoui A, Steiner ML, Weber A, Abou-Ras D, Kotschau I, et al. (2009) Cu_2ZnSnS_4 thin film solar cells from electroplated precursors: Novel low cost perspective. Thin Solid Films 517: 2511-2514.
3. Hironori K, Kotoe S, Tsukasa W, Hiroyuki S, Tomomi K, et al. (2001) Development of thin film solar cell based on Cu_2ZnSnS_4 thin films. Sol Energy Mater Sol Cells 65: 141-148.
4. Jonathan JS, Dominik MB, Philip JD (2010) A 3.2% efficient Kesterite device from electrodeposited stacked elemental layers. J Electroanal Chem 646: 52-59.
5. Kazuo J, Ryoichi K, Tsuyoshi K, Satoru Y, Win SM, et al. (2007) Cu_2ZnSnS_4 type thin film solar cells using abundant materials. Thin Solid Films 515: 5997-5999.
6. Chalapathy RBV, Jung GS, Ahn BT (2011) Fabrication of Cu_2ZnSnS_4 films by sulfurization of Cu/ZnSn/Cu precursor layers in sulfur atmosphere for solar cells. Sol Energy Mater Sol Cells 95, 3216-3221.
7. Schubert B, Marsen B, Cinque S, Unold T, Klenk R, et al. (2011) Cu_2ZnSnS_4 thin film solar cells by fast co-evaporation. Prog Photovolt: Res Appl 19: 93-96.
8. Shinde NM, Dubal DP, Dhawale DS, Lokhande CD, Kim JH, et al. (2012) Room temperature novel chemical synthesis of Cu_2ZnSnS_4 (CZTS) absorbing layer for photovoltaic application. Mater Res Bull 47: 302-307.
9. Tsukasa W, Tomokazu S, Shin T, Tatsuo F, Tomoyoshi M, et al. (2012) 6% efficiency Cu_2ZnSnS_4 based thin film solar cells using oxide precursors by open atmosphere type CVD. J Mater Chem 22: 4021-4024.
10. Wang K, Gunawan O, Todorov T, Shin B, Chey SJ, et al. (2010) Thermally evaporated Cu_2ZnSnS_4 solar cells. Appl Phys Lett 97: doi: http://dx.doi.org/10.1063/1.3499284.
11. Ho SM, Anuar K, Tan WT, (2013) Thickness dependent characteristics of chemically deposited tin sulfide films. Universal J Chem 1: 170-174.

12. Anuar K, Ho SM, Nagalingam S, Tan WT, Darren T, (2010) Chemical bath deposition of nickel sulphide (Ni_4S_3) thin films. Leonardo J Sci 16: 1-12.

13. Ezema FI, Ekwealor ABC, Asogwa PU, Ugwuoke PE, Chigbo C, et al. (2007) Optical properties and structural characterizations of Sb_2S_3 thin films deposited by chemical bath deposition technique. Turk J Phys 31: 205-210.

14. Ezema FI, Ekwealor ABC, Osuji RU (2006) Effect of thermal annealing on the band GAP and optical properties of chemical bath deposited ZnSe thin films. Turk J Phys 30: 157-163.

15. Ho SM, Anuar K, Atan S, Saravanan N (2010) X-ray diffraction and atomic force microscopy studies of chemical bath deposited FeS thin films. Studia UBB Chemia 55: 5-11.

16. Kassim A, Ho SM, Tan WT, Ngai CF (2011) Influence of triethanolamine on the chemical bath deposited NiS thin films. Am J Appl Sci 8: 359-361.

17. Oztas M, Bedir M, Bakkaloglu OF, Ormanci R (2005) Effect of Zn:Se ratio on the properties of sprayed ZnSe thin films. Acta Phys Pol A 107: 525-534.

18. Raniero L, Ferreira CL, Cruz LR, Pinto AL, Alves RM (2010) Photoconductivity activation in PbS thin films grown at room temperature by chemical bath deposition. Phys B: Condens Matter 405: 1283-1286.

19. Wei AX, Zhao XH, Liu J, Zhao Y (2013) Investigation on the structure and optical properties of chemically deposited ZnSe nanocrystalline thin films. Phys B 410: 120-125.

20. Alaa AA (2013) The structural and optical properties of nonstoichiometric $AgAlS_2$ thin films prepared by chemical spray pyrolysis method. Tikrit J Pure Sci 18: 145-149.

21. Alias MFA, Naji S, Taher BY (2014) Influence of substrate temperatures on the optical properties of thin Cu_3SnS_4 films prepared by CBD. IPASJ Int J Electr Eng 2: 1-7.

22. Chaudhari JB, Deshpande NG, Gudage YG, Ghosh A, Huse VB, Sharma R (2008) Studies on growth and characterization of ternary $CdS_{1-x}Se_x$ alloy thin films deposited by chemical bath deposition technique. Appl Surf Sci 254: 6810–6816.

23. Haron MJ, Ho SM, Anuar K, Tan WT, Atan S, et al. (2009) Effect of deposition period and bath temperature on the properties of electrodeposited Cu_4SnS_4 films. Solid State Sci Technol 17: 226-237.

24. Deshmukh LP, Mane ST, Lendave SA, Pingale PC, Suryawanshi RV, et al. (2012) Photovoltaic studies of $Cd_{1-x}Co_xS$ based electrochemical cells. J Nepal Chem Soc 30: 151-158.

25. Ho SM (2014) Influence of complexing agent on the growth of chemically deposited $Ni_3Pb_2S_2$ thin films. Oriental J Chem 30: 1009-1012.

26. Kassim A, Ho SM, Tan WT, Saravanan N (2010) Composition, structure and photoelectrochemical characterization of electrodeposited Cu_4SnS_4 thin films. Oriental J Chem 26: 389-394.

27. Mahapatra PK, Panda BB (2015) Photoelectrochemical cells using electrosynthesized cadmium sulphide and mixed sulphide of bismuth (III) and cadmium (II) as photoelectrodes. Int J Thin Films Sci Technol 4: 45-49.

28. Manauti MS, Patil SM, Mane RM, Patil SV, Bhosale PN (2012) Photoelectrochemical cell performance of chemically deposited $MoBi_2Te_5$ thin films. Adv Mater Lett 3: 71-76.

29. Mehrez NB, Khemiri N, Kanzari M (2016) Study of structural and morphological properties of thermally evaporated $Sn_2Sb_6S_{11}$ thin films. Mater Chem Phys 182: 133-138.

30. More PD, Shahane GS, Deshmukh LP, Bhosale PN (2003) Spectro-structural characterization of $CdSe_{1-x}Te_x$ alloyed thin films. Mater Chem Phys 80: 48-54.

31. Mutlu K (2011) The annealing effect on structural, optical and photoelectrical properties of $CuInS_2/In_2S_3$ films. Phys B: Condens Matter 406: 2953-2961.

32. Shadia JI, Hassan KJ, Riyad N (2013) Nanocrystalline CdS: In thin films prepare by the spray pyrolysis technique. J Lumin 141: 27-32.

33. Subramanian B, Sanjeeviraja C, Jayachandran M (2003) Materials properties of electrodeposited $SnS_{05}Se_{05}$ films and characterization of photoelectrochemical solar cells. Mater Res Bull 38: 899-908.

34. Tan WT, Ho SM, Anuar K, Atan S, Haron MJ, et al. (2008) Effects of bath temperature on the electro deposition of Cu_4SnS_4 thin films. J Appl Sci Res 4: 1701-1707.

35. Jeong J, Park G (2003) Structural and Electrical Properties of $CuGaS_2$ Thin Films by Electron Beam Evaporation. Sol Energy Mater Sol Cells 75: 93-100.

36. Yeh L, Cheng K (2015) Preparation of chemical bath synthesized ternary Ag-Sn-S thin films as the photoelectrodes in photoelectrochemical cell. J Power Sources 275: 750-759.

37. Bushra AH, Muthafar FA, Duaa AU (2011) The optical properties of (CuInSTe) thin films. Al-Mustansiriyah J Sci 22: 211-221.

38. Bwamba A, Alu N, Adama K, Abdullahi Z, Iwok U, et al. (2014) Characterization of CZTS absorbent material prepared by field assisted spray pyrolysis. Am J Mater Sci 4: 127-132.

39. Chen YS, Wang YJ, Li R, Gu JH, Lu JX, et al. (2012) Preparing Cu_2ZnSnS_4 films using the co-electro deposition method with ionic liquids. Chin Phys B 21: 058801.

40. Colantoni A, Longo L, Boubaker K (2014) Structural investigation of photocatalyst solid $Ag_{1-x}Cu_xInS_2$ quaternary alloys sprayed thin films optimized within the lattice compatibility theory scope. J Mater 1-5. http://dxdoiorg/101155/2014/325271

41. Kentaro I, Tatsuo N (1988) Electrical and optical properties of stannite type quaternary semiconductor thin films. Jpn J Appl Phys 27: doi:101143/JJAP272094.

42. Lin XZ, Kavalakkatt J, Kornhuber K, Levcenko S, Lux-Steiner MC, et al. (2013) Structural and optical properties of Cu_2ZnSnS_4 thin films absorbers from ZnS and Cu_3SnS_4 nanoparticle precursors. Thin Solid Films 535: 10-13.

43. Jiang H, Wei X, Huang Y, Wang X, Han A, et al. (2017) Achieving composition controlled Cu_2ZnSnS_4 films by sulfur free annealing process. Jpn J Appl Phys 56: https://doi.org/10.7567/JJAP.56.065502.

44. Patil SP, Mane RM, Kharade RR, Mali SS, Bhosale PN (2012) Novel synthetic route for quaternary $MoBiGaSe_5$ mixed metal chalcogenide (MMC) thin films. Dig J Nanomater Biostruct 7, 237-245.

45. Peng CY, Dhakal TP, Garner S, Cimo P, Lu S, et al. (2014) Fabrication of Cu_2ZnSnS_4 solar cell on a flexible glass substrate. Thin Solid Films 562: 574-577.

46. Subramaniam EP, Rajesh G, Muthukumarasamy N, Thambidurai M, Asokan V, et al. (2014) Solar cells of Cu_2ZnSnS_4 thin films prepared by chemical bath deposition method. Indian J Pure Appl Phys 52: 620-624.

47. Xie M, Zhuang DM, Zhao M, Zhuang ZL, Ouyang LQ, et al. (2013) Preparation and characterization of Cu_2ZnSnS_4 thin films and solar cells fabricated from quaternary Cu-Zn-Sn-S target. Int J Photoenergy: doiorg/101155/2013/929454

48. Yeh LY, Cheng KW (2014) Preparation of the Ag-Zn-Sn-S quaternary photoelectrodes using chemical bath deposition for photoelectrochemical applications. Thin Solid Films 558: 289-293.

49. Ingo R, Jan K, Jurgen P, Thomas D, Alejandro A (2014) One dimensional simulation of sequentially processed $Cu(In_{1-x}Ga_x)(Se_{1-y}S_y)$ heterojunction solar cells with vertically graded absorber composition. Phys B: Condens Matter 439: 9-13.

50. Keller J, Schlesiger R, Riedel I, Parisi J, Schmitz G, et al. (2013) Grain boundary investigations on sulfurized $Cu(In,Ga)(S,Se)_2$ solar cells using atom probe tomography. Sol Energy Mater Sol Cells 117, 592-598.

51. Mario G, William NS (2005) Five source PVD for the deposition of $Cu(In_{1-x}Ga_x)(Se_{1-y}S_y)_2$ absorber layers. Thin Solid Films 480-481: 33-36.

52. Richter M, Schubbert C, Eraerds P, Riedel I, Keller J, et al. (2013) Optical characterization and modeling of $Cu(In,Ga)(Se,S)_2$ solar cells with spectroscopic ellipsometry and coherent numerical simulation. Thin Solid Films 535: 331-335.

53. Taunier S, Sicx J, Grand PP, Chomont A, Ramdani O (2005) $Cu(In,Ga)(S,Se)_2$ solar cells and modules by electrodeposition. Thin Solid Films 480-481: 526-531.

54. Anuar K, Ho SM, Tan WT, Atan MS, Dzulkefly K, et al. (2007) Cyclic voltammetry study of copper tin sulphide compounds. Pacific J Sci Technol 8: 252-260.

55. Ali AM, Inokuma T, Hasegawa S (2006) Structural and Photo-luminescence properties of nanocrystalline silicon films deposited at low temperature by plasma-enhanced chemical vapor deposition. Appl Surf Sci 253: 1198-1204.

56. Armstrong S, Datta PK, Miles RW (2002) Properties of zinc sulfur selenide deposited using a close-spaced sublimation method. Thin Solid Films 403-404: 126-129.

57. Atan S, Tan WT, Anuar K, Ho SM (2010) Influence of triethanolamine on the properties of chemical bath deposited nickel sulphide thin films. Jurnal Nanosains & Nanoteknologi 3: 22-24.

58. Berrigan RA, Maung N, Irvine S, Cole-Hamilton D, Ellis D (1998) Thin films of CdTe/CdS grown by MOCVD for photovoltaics. J Cryst Growth 195: 718-724.

59. Cheng SY, Chen GN, Chen YQ, Huang CC (2006) Effect of deposition potential and bath temperature on the electrodeposition of SnS film. Opt Mater 29: 439-444.

60. Gautier C, Breton G, Nouaoura M, Cambon M, Charar S, et al. (1998) Sulfide films on PbSe thin layer grown by MBE. Thin Solid Films 315: 118-122.

61. Medina MJ, Torres J, Olaizola JL, Alcantara JM, Hancik V, et al. (2016) Synthesis of europium doped ZnS nano crystalline thin films with strong blue photoluminescence. RSC Adv 6: 107613-107621.

62. Guillen C, Martinez MA, Herrero J, Gutierrez MT (1999) Chemical studies of solar cell structures based on electrodeposited $CuInSe_2$. Sol Energy Mater Sol Cells 58: 219-224.

63. Gupta A, Parikh V, Compaan AD (2006) High efficiency ultra-thin sputtered CdTe solar cells. Sol Energy Mater Sol Cells 90: 2263-2271.

64. Ion L, Antohe S, Popescu M, Scarlat F, Sava F, et al. (2004) Structure and electrical properties of electron irradiated CdSe thin films. J Optoelectron Adv Mater 6: 113-119.

65. Kassim A, Ho SM, Abdul HA, Saravanan N (2010) Influence of the deposition time on the structure and morphology of the ZnS thin films electrodeposited on indium tin oxide substrates. Dig J Nanomater Biostruct 5: 975-980.

66. Kumar S, Sharma TP, Zulfequar M, Husain M (2003) Characterization of vacuum evaporated PbS thin films. Phys B: Condens Matter 325: 8-16.

67. Nishino J, Chatani S, Uotani Y, Nosaka Y (1999) Electrodeposition method for controlled formation of CdS films from aqueous solutions. J Electroanal Chem 473: 217-222.

68. Oja I, Nanu M, Katerski A, Krunks M, Mere A, et al. (2005) Crystal quality studies of $CuInS_2$ films prepared by spray pyrolysis. Thin Solid Films 480-481: 82-86.

69. Om PS, Nadarajah M, Kuldeep SG, Rahul P, Manas D, et al. (2016) Effect of sputter deposited Zn precursor film thickness and annealing time on the properties of Cu_2ZnSnS_4 thin films deposited by sequential reactive sputtering of metal targets. Mater Sci Semicond Process 52: 38-45.

70. Pistone A, Arico AS, Antonucci PL, Silvestro D, Antonucci V (1998) Preparation and characterization of thin film ZnCuTe semiconductors. Sol Energy Mater Sol Cells 5: 255-267.

71. Purohit A, Chander S, Nehra SP, Lal C, Dhaka MS (2016) Thickness dependent optical and electrical properties of CdSe thin films. AIP Conf Proc doi: http://dxdoiorg/101063/14946642.

72. Rizzo A, Tagliente MA, Caneve L, Scaglione S (2000) The influence of the momentum transfer on the structural and optical properties of ZnSe thin films prepared by rf magnetron sputtering. Thin Solid Films 368: 8-14.

73. Saloniemi H, Kemell M, Ritala M, Leskela M (2001) Electrochemical quartz crystal microbalance study on cyclic electrodeposition of PbS thin films. Thin Solid Films 386: 32-40.

74. Saravanan N, Anuar K, Ho SM, Koon KL, Tan WT (2010) Effect of pH value and electrolyte concentration on the copper sulphide thin films prepared by chemical bath deposition method. Gazi Univ J Sci 23: 435-443.

75. Shen CM, Zhang XG, Li HL (2001) Effect of pH on the electrochemical deposition of cadmium selenide nanocrystal films. Mater Sci Eng B 84: 265-270.

76. Soliman M, Kashyout AB, Shabana M, Elgamal M (2001) Preparation and characterization of thin films of electrodeposited CdTe semiconductors. Renew Energy 23: 471-481.

77. Tan WT, Anuar K, Ho SM, Shanthi S, Saravanan N, Haron MJ, Dzulkefly KA (2010) Preparation and characterization of PbSe thin films by chemical bath deposition. Jurnal Kimia 4: 1-6.

78. Timoumi A, Bouzouita H, Kanzari M, Rezig B (2005) Fabrication and characterization of In_2S_3 thin films deposited by thermal evaporation technique. Thin Solid Films 480-481: 124-128.

79. Vivet N, Doualan JL, Morales M, Levalois M (2010) Luminescence properties of Cr^{2+}:ZnSe: comparison between an single crystal and a film deposited by RF magnetron co-sputtering. J Lumin 130: 1449-1454.

80. Wijesundera RP, Siripala W (2004) Preparation of $CuInS_2$ thin films by electrodeposition and sulphurisation for applications in solar cells. Sol Energy Mater Sol Cells 81: 147-154.

81. Aadim KA, Ibrahim AE, Marie JM (2017) Structural and optical properties of PbS thin films deposited by pulsed laser deposited (PLD) technique at different annealing temperature. Int J Phys 5: 1-8.

82. Anuar K, Ho SM, Haron MJ, Nagalingam S (2011) Preparation of thin films of copper sulfide by chemical bath deposition. Int J Pharm Life Sci 2: 1190-1194.

83. Chtouki T, Kouari YE, Kulyk B, Louardi A, Rmili A, et al. (2017) Spin coated nickel doped cadmium sulfide thin films for third harmonic generation applications. J Alloys Compd 696: 1292-1297.

84. Gedi S, Reddy VRM, Pejjai B, Park C, Jeon C, Kotte TR (2017) Studies on chemical bath deposited SnS_2 films for Cd-free thin film solar cells. Ceram Int 43: 3713-3719.

85. Fernandez A, Navarrete C, Valenzuela P, Gacitua W, Mosquera E, et al. (2017) Characterization of chemically deposited aluminium doped CdS thin films with post deposition thermal annealing. Thin Solid Films 623: 127-134.

86. Gremenok VF, Martin RW, Bodnar IV, Yakushev MV, Schmitz W, et al. (2001) Characterization of polycrystalline $Cu(In,Ga)Te_2$ thin films prepared by pulsed laser deposition. Thin Solid Films 394: 23-28.

87. Ho SM (2016) A brief review of the growth of pulsed laser deposited thin films. British J Appl Sci Technol 14: 1-6.

88. Ho SM (2016) Metal selenide semiconductor thin films: a review. Int J ChemTech Res 9: 390-395.

89. Ho SM (2016) A review on the sputtering deposition film growth. J Appl Sci Res 12: 44-48.

90. Ho SM (2016) Synthesis of thin films on flexible substrates: a review. Middle East J Sci Res 24: 2235-2238.

91. Jeong W, Park G (2004) Structural and electrical characterization of $CuInS_2$ thin films by stacked elemental layer (SEL) method. J Korean Phys Soc 45: S534-S537.

92. Kassim A, Ho SM, Loh YY, Tan WT, Nagalingam S (2012) Complexing agent effect on the properties of iron sulphide thin films. Can J Pure Appl Sci 6: 1863-1867.

93. Khemiri N, Khalfallah B, Abdelkader D, Kanzari M (2014) X-ray diffraction spectroscopy studies of $CuIn_{2n+1}S_{3n+2}$ thin films. Int J Thin Films Sci Technol 3: 7-12.

94. Lin Y, Chi Y, Hsieh T, Chen Y, Huang K (2016) Preparation of Cu_2ZnSnS_4 (CZTS) sputtering target and its application to the fabrication of CZTS thin film solar cells. J Alloys Compd 654: 498-508.

95. Om PS, Parmar R, Gour KS, Dalai MK, Tawale J, et al. (2015) Synthesis and characterization of petal type CZTS by stacked layer reactive sputtering. Superlattices Microstruct 88: 281-286.

96. Ma L, Ai X, Wu X (2017) Effect of substrate and Zn doping on the structural, optical and electrical properties of CdS thin films prepared by CBD method. J Alloys Compd 691: 399-406

97. More PD (2012) Synthesis and characterization of hydrophobic PbS thin films. Adv Appl Sci Res 3: 2508-2513.

98. Moreno OP, Lima LA, Portillo MC, Castilla SR, Tototzintle MZ, Et al. (2012) Properties of PbS: Ni^{2+} nanocrystals in thin films by chemical bath deposition. ISRN Nanotechnol http://dxdoiorg/105402/2012/546027.

99. Nanu M, Reijnen L, Meester B, Schoonman J, Goossens A (2004) $CuInS_2$ thin films deposited by ALD. Chem Vapor Deposition 10: DOI: 101002/cvde200306262.

100. Roy S, Guha P, Chaudhuri S, Pal AK (2002) $CuInTe_2$ thin films synthesized by graphite box annealing of In/Cu/Te stacked elemental layers. Vacuum 65: 27-37.

101. Simone DM, Daniele M, Andrei S, Elisa A, Fabio P, et al. (2017) SnS thin film solar cells: Perspectives and limitations. Coatings 7: doi:103390/coatings7020034

102. Vanalakar SA, Agawane GL, Shin SW, Suryawanshi MP, Gurav KV, et al. (2015) A review on pulsed laser deposited CZTS thin films for solar cell applications. J Alloys Compd 619: 109-121.

103. Zhang W, Zhu H, Zhang L, Guo Y (2017) $Cu(In,Ga)Se_2$ thin film solar cells grown at low temperatures. Solid State Electron 132: 57-63.

104. Antony A, Murali KV, Manoj R, Jayaraj MK (2005) The effect of the pH value on the growth and properties of chemical bath deposited ZnS thin films. Mater Chem Phys 90: 106-110.

105. Anuar K, HO SM, Tan WT, Nagalingam S (2011) Deposition and characterization of ZnS thin films using chemical bath deposition method in the presence of sodium tartrate as complexing agent. Pak J Sci Ind Res 54: 1-5.

106. Apolinar A, Acosta MC, Quevedo MA, Ramirez R, Leon A, et al. (2011) Acetylacetone as complexing agent for CdS thin films grow chemical bath deposition. Chalcogenide Lett 8: 77-82.

107. Arepalli VK, Challa KK, Kim E (2015) Effects of complexing agents on the chemical bath deposition of uniform Cu_2ZnSnS_4 thin films. Nanosci Nanotechnol Lett 7: 729-733.

108. Carrillo A, Lazaro RCA, Perez A, Martinez CA, Terrazas EC, et al. (2014) Role of complexing agents in chemical bath deposition of lead sulfide thin films. Mater Lett 121: 19-21.

109. Castillo A, Lazaro RCA, Ojeda EL, Perez CAM, Lopez MAQ, et al. (2013) Characterization fof CdS thin films deposited by chemical bath deposition using novel complexing agents. Chalcogenide Lett 10: 421-425.

110. Chaitali SB, Vishvanath BG, Suvarta DK, Khot KV, Kharade RR, et al. (2016) Rapid formation of ternary $CdZnSe_2$ chalcogenide thin film by microwave assisted chemical bath deposition. Macromol Symp 362: 60-64.

111. Chen L, Zhang D, Chen Q (2006) The effects of the complexing agents on the growth and properties of modified chemical bath deposited ZnS thin films. 2006 1st IEEE International Conference on Nano/Micro engineered and molecula systems, Zhuhai, 2006 599-602 DOI: 101109/NEMS2006334853.

112. Chidozie O (2015) The growth and characterization of copper sulphide thin film using CBD (Chemical bath deposition) technique. J Mater Sci Eng B 5: 181-186.

113. Deshpande MP, Garg N, Bhatt SV, Sakariya P, Chaki SH (2013) Spectroscopy and structural study on CdSe thin films deposited by chemical bath deposition. Adv Mater Lett 4: 869-874.

114. Ezenwa IA, Elekalachi CI (2015) Transmittance spectra of CuS thin film at varying concentration of complexing agent. Int J Mater Chem Phys 1: 281-285.

115. Goverdhan Y, Pathak KK, Deshmukh K, Pateria MA (2015) Studies on optical and structural properties of Ag_2S films prepared by chemical bath deposition method. Int J Multidisciplinary Res Mod Educ: 296-301.

116. Ho SM (2015) Scanning electron microscopy study of surface morphology of $Ni_3Pb_2S_2$ thin films. Asian J Chem 27: 3851-3853.

117. Johnston D, Carletto MH, Reddy KTR, Forbes I, Miles RW (2002) Chemical bath deposition of zinc sulfide based buffer layers using low toxicity materials. Thin Solid Films 403-404: 102-106.

118. Kassim A, Ho SM, Saravanan N, Kuang Z, Tan WT (2010) Influence of complexing agent (Na_2EDTA) on chemical bath deposited Cu_4SnS_4 thin films. Bull Chem Soc Ethiopia 24: 259-266.

119. Khallaf H, Oladeji IO, Chow L (2008) Optimization of chemical bath deposited CdS thin films using nitrilotriacetic acid as a complexing agent. Thin Solid Films 516: 5967-5973.

120. Ladar M, Popovici EJ, Baldea I, Grecu R, Indrea E (2007) Studies on chemical bath deposited zinc sulphide thin films with special optical properties. J Alloys Compd 434-435: 697-700.

121. Long F, Wang WM, Cui ZK, Fan LZ, Zou ZG, et al. (2008) An improved method for chemical bath deposition of ZnS thin films. Chem Phys Lett 462: 84-87.

122. Mathew X, Enriquez JP (2003) Influence of the thickness on structural, optical and electrical properties of chemical bath deposited CdS thin films. Sol Energy Mater Sol Cells 76: 313-322.

123. Mendoza-Perez R, Santana-Rodriguez G, Sastre-Hernandez J, Morales-Acevedo A, Arias-Carbajal A, et al. (2005) Effects of thiourea concentration on CdS thin films grown by chemical bath deposition for CdTe solar cells. Thin Solid Films 480-481: 173-176.

124. Nasr TB, Kamoun N, Guasch C (2006) Structure, surface composition and electronic properties of zinc sulphide thin films. Mater Chem Phys 96: 84-89.

125. Okereke NA (2015) Effect of dip time structural and optical properties of $CuAlSe_2$ films. Int Educ Sci Res J 1: 34-36.

126. Pradhan B, Sharma AK, Ray AK (2007) Conduction studies on chemical bath deposited nano crystalline CdS thin films. J Cryst Growth 304: 388-392.

127. Preetha KC, Deepa K, Dhanya AXC, Remadevi TL (2015) Role of complexing agents on chemical bath deposited PbS thin film characterization. IOP Conf Series: Mater Sci Eng 73: doi 101088/1757-899X/73/1/012086.

128. Roy P, Srivastava SK (2006) In situ deposition of Sn doped CdS thin films by chemical bath deposition and their characterization. J Phys D: Appl Phys 39: 4771-4776.

129. Sengupta S, Perez M, Rabkin A, Golan Y (2016) In situ monitoring the role of citrate in chemical bath deposition of PbS thin films. Cryst Eng Comm 18: 149-156.

130. Seung WS, Agawane GL, Myeng GG, Moholkar AV, Jong HM, et al. (2012) Preparation and characteristics of chemical bath deposited ZnS thin films: Effect of different complexing agents. J Alloys Compd 526: 25-30.

131. Sonawane PS, Wani PA, Patil LA, Seth T (2004) Growth of $CuBiS_2$ thin films by chemical bath deposition technique from an acidic bath. Mater Chem Phys 84: 221-227.

132. Zhang H, Ma X, Yang D (2004) Effects of complexing agent on CdS thin films prepared by chemical bath deposition. Mater Lett 58: 5-9.

133. Anuar K, Ho SM, Mohd YR (2011) UV-Visible studies of chemical bath deposited NiSe thin films. Int J Chem Res 3: 21-26.

134. Betkar MM, Bagde GD (2012) Structural and optical properties of spray deposited CdSe thin films. Mater Phys Mech 14: 74-77.

135. Buba ADA, Umar M, Gurku MU (2016) Temperature dependence of optical properties of PbSe thin films. IOSR J Appl Phys 8: 56-61.

136. Chandra SK, Shekar GL, Krishnamurthy L, Urs RG (2014) Surface morphological studies of solar absorber layer Cu_2ZnSnS_4 (CZTS) thin films by non-vacuum deposition methods. J Nano Electron Phys 6: 02004-1 to 02004-5

137. Dwivedi DK, Nitesh S, Pathak HP, Kedar S (2014) Structural and optical properties of different composition of $Se_{90}Cd_{10-x}In_x$ thin films by vacuum evaporation technique. Am J Mater Sci Eng 2: 13-17.

138. Geetha G, Priya M, Suresh S (2017) Optical and electrical properties of chemical bath deposited cobalt sulphide thin films. Mater Res 20: 62-67.

139. Hajar F, Amir AY, Mehdi HS, Alimorad R, Asghar KZ (2016) Control of morphology and optical properties of PbS nanostructured thin films by deposition parameters: study of mechanism. J Exp Nanosci 11: http://dxdoiorg/101080/1745808020161237054.

140. Ibrahim SG, Ubale AU (2014) Size dependent physical properties of spray deposited nanocrystalline $Cd_{05}Fe_{05}Se$ thin films. Int J Mater Chem 4: 1-8.

141. Isi PO, Ekwo PI (2013) Growth and characterization of lead selenide (PbSe) thin film by chemical bath deposition. Res J Eng Sci 2: 15-19.

142. Kassim A, Ho SM, Abdullah AH, Nagalingam S (2010) XRD, AFM and UV-Vis optical studies of PbSe thin films produced by chemical bath deposition method. Sci Iranica 17: 139-143.

143. Logu T, Sankarasubramanian K, Soundarrajan P, Sampath M, Sethuraman K (2014) Hydrophobic CdSe:Sb thin films by chemical spray pyrolysis technique. Int J Sci Res Conference on Advanced Technology Oriented Materials (ATOM-2014), 8-9th Dec-2014, 36-39.

144. Meshram RS, Thombre RM (2015) Structural and optical properties of CdSe thin films prepared by spray pyrolysis technique. Int J Adv Sci Eng Technol 1: 167-170.

145. Narayana S, Pushpalatha HL, Ganesha R (2017) Synthesis of CdSe thin film by chemical bath deposition and characterization. Int J Eng Sci Inno Technol 6: 41-49.

146. Patel KD, Jani MS, Pathak VM, Srivastava R (2009) Deposition of CdSe thin films by thermal evaporation and their structural and optical properties. Chalcogenide Lett 6: 279-286.

147. Subhash C, Dhaka MS (2015) Preparation and physical characterization of CdTe thin films deposited by vacuum evaporation for photovoltaic applications. Adv Mater Lett DOI: 105185/amlett20155926.

148. Tan WT, Ho SM, Anuar K, Abdul HA, Ahmad HJ, et al. (2010) Effect of solution concentration on MnS_2 thin films deposited in a chemical bath. Kasetsart J: Nat Sci 44: 446-453.

149. Veena E, Kasturi VB, Shivakumar GK (2016) Influence of lead precursor concentration on properties of spray deposited lead sulphide thin films. Int J Pure Appl Phys 12: 97-112.

150. Vishwakarma SR, Kumar A, Prasad S, Tripathi RS (2013) Synthesis and characterization of n-CdSe thin films deposited at different substrate temperatures. Chalcogenide Lett 10: 393-402.

151. Akl AA, Hassanien AS (2015) Microstructure and crystal imperfections of nanosized CdS_xSe_{1-x} thermally evaporated thin films. Superlattices Microstruct 85: 67-81.

152. Farha YS, Shaheed US, Deepali JD, Deepak SU (2014) Band gap engineering by substitution of S by Se in nanostructured $CdS_{1-x}Se_x$ thin films grown by soft chemical route for photosensor application. Mater Sci Semicond Process 27: 404-411.

153. Anuroop R, Pradeep B (2017) Structural, optical, ac conductivity and dielectric relaxation studies of reactively evaporated In_6Se_7 thin films. J Alloys Compd, 702: 432-441.

154. Bari RH, Patil LA (2010) Synthesis and characterization of bismuth selenide thin films by chemical bath deposition technique. Indian J Pure Appl Phys 48: 127-132.

155. Barote MA, Yadav AA, Masumdar EU (2011) Effect of deposition parameters on growth and characterization of chemically deposited $Cd_{1-x}Pb_xS$ thin films. Chalcogenide Lett 8: 129-138.

156. Chander S, Dhaka MS (2017) Thermal annealing induced physical properties of electron beam vacuum evaporated CdZnTe thin films. Thin Solid Films 625: 131-137.

157. Dedova T, Krunks M, Volobujeve O, Oja I (2005) ZnS thin films deposited by spray pyrolysis technique Phys Status Solidi C 2: 1161-1166.

158. Dhanam M, Prabhu RR, Manoj PK (2008) Investigations on chemical bath deposited cadmium selenide thin films. Mater Chem Phys 107: 289-296.

159. Dong HH, Jung HA, Kwun NH, Kwan SH, Young GS (2012) Structural and optical properties of ZnS thin films deposited by RF magnetron sputtering. Nanoscale Res Lett 7: 26.

160. Gode F, Gumus C, Zor M (2007) Investigations on the physical properties of the polycrystalline ZnS thin films deposited by the chemical bath deposition method. J Cryst Growth 299: 136-141.

161. Gumus C, Ulutas C, Esen R, Ozkendir OM, Ufuktepe Y (2005) Preparation and characterization of crystalline MnS thin films by chemical bath deposition. Thin Solid Films, 492: 1-5.

162. Ho SM (2016) Application of energy dispersive X-ay analysis technique in chalcogenide metal thin films: review. Middle East J Sci Res 24: 445-449.

163. Ho SM, Anuar K, Saravanan N, Kim KS (2011) SEM, EDAX and UV-visible studies on the properties of Cu_2S thin films. Chalcogenide Lett 8: 405-410.

164. Kalyanasundaram S, Panneerselvam K, Kumar VS (2013) Study on physical properties of ZnS thin films prepared by chemical bath deposition. Asia Pacific J Res 1: 5-14.

165. Lokhande CD, Sankapal BR, Mane RS, Pathan HM, Muller M, et al. (2002) XRD, SEM, AFM, HRTEM, EDAX and RBS studies of chemically deposited Sb_2S_3 and Sb_2Se_3 thin films. Appl Surf Sci 193: 1-10.

166. Mali SS, Shinde PS, Betty CA, Bhosale PN, Oh YW, et al. (2012) Synthesis and characterization of Cu_2ZnSnS_4 thin films by SILAR method. J Phys Chem Solids 73: 735-740.

167. Mathuri S, Ramamurthi K, Babu RR (2017) Influence of deposition distance and substrate temperature on the CdSe thin films deposited by electron beam evaporation technique. Thin Solid Films 625: 138-147.

168. Memon AA, Dilshad M, Revaprasadu N, Malik MA, Raftery J, et al. (2015) Deposition of cadmium sulfide and zinc sulfide thin films by aerosol assisted chemical vapors from molecular precursors. Turk J Chem 39: 169-178.

169. Patel TH (2012) Influence of deposition time on structural and optical properties of chemically deposited SnS thin films. The Open Surf Sci J 4: 6-13.

170. Ozakin O, Betul G, Yildirim M, Musfata S (2012) Influence of film thickness on structural and optical properties of ZnS thin films obtained by SILAR method and analysis of Zn/ZnS/n-GaAs/In sandwich structure. Phys Status Solidi A 209: 687-693.

171. Sachin R, Avinash R, Adinath F, Moses K, Habib P, et al. (2017) Synthesis of CdS thin films at room temperature by RF magnetron sputtering and study of its structural, electrical, optical and morphology properties. Thin Solid Films 631: 41-49.

172. Santhosh TCM, Bangera KV, Shivakumar GK (2017) Band gap engineering of mixed $Cd_{(1-x)}Zn_{(x)}Se$ thin films. J Alloys Compd 703: 40-44.

173. Kazuya M, Kunihiko T, Yuya N, Hisao U (2010) Annealing temperature dependence of properties of Cu_2ZnSnS_4 thin films prepared by sol gel sulfurization method. Jpn J Appl Phys 50: https://doi.org/10.1143/JJAP.50.05FB08.

174. Xu P, Xu G, Chu K, Wang N, Zhou Q, et al. (2013) Properties study of ZnS thin films deposited on HgCdTe substrate by different methods. Proc of the SPIE, Volume 8907: id 890742, DOI 101117/122034530.

175. Sunil HC, Sanjaysinh MC, Jiten PT, Milind PD (2017) Synthesis of manganese sulfide (MnS) thin films by chemical bath deposition and their characterization. J Mater Res Technol 6: 123-128.

176. Sunil HC, Kanchan SM, Tasmira JM, Deshpande MP (2017) $CuAlS_2$ thin films-dip coating deposition and characterization. J Sci: Adv Mater Devices 2: 215-224.

177. Veena E, Kasturi VB, Shivakumar GK (2017) Effective role of thickness on structural, electrical and optical properties of lead sulphide thin films for photovoltaic applications. Mater Sci Eng B 223: 64-69.

178. Subhash C, Purohit A, Lal C, Dhaka MS (2017) Enhancement of optical and structural properties of vacuum evaporated CdTe thin films. Mater Chem Phys 185: 202-209.

179. Priya K, Ashith VK, Rao GK, Ganesh S (2017) A comparative study of structural, optical and electrical proeprties of ZnS thin films obtained by thermal evaporation and SILAR techniques. Ceram Int 43: 10487-10493.

180. Subhash C, Dhaka MS (2016) Optimization of structural, optical and electrical properties of CdZnTe thin films with the application of thermal treatment. Mater Lett 182: 98-101.

181. Somnath M, Asit KK (2017) The effect of annealing on structural, optical and photosensitive properties of electrodeposited cadmium selenide thin films. J Sci: Adv mater Devices 2: 165-171.

182. Vallem S, Kasturi VB, Shivakumar GK (2017) Effect of substrate temperature and film thickness on the thermoelectric properties of In_2Te_3 thin films. J Alloys Compd 715: 224-229.

183. Kotb MS, Jumana ZA, Kotkata MF (2017) Investigation on microstructural and optical properties of nano crystalline CdSe thin films. Thin Solid Films 631: 219-226.

184. Astam A (2016) Structural and optical characterization of Cu_2SnSe_3 thin films prepared by SILAR method. Thin Solid Films 615: 324-328.

185. Priya SS, Shree BL, Ranjani PT, Karthick P, Jeyadheepan K, et al. (2016) Electrical properties of thermally evaporated CdSe and ZnCdSe thin films. Mater Today: Proc 3: 1487-1493.

186. Hone FG, Ampong FK (2016) Effect of deposition temperature on the structural, morphological and optical band gap of lead selenide thin films synthesized by chemical bath deposition method. Mater Chem Phys 183: 320-325.

187. Selvakumar C, Venkatachalam T, Kumar ER (2016) Preparation, characterization and ab-initio study of $CdSnTe_2$ thin films by closed space sublimation technique. Superlattices Microstruct 90: 38-44.

188. Hemalatha S, Tamil I, Rachel O, Usha R (2016) Marigold microstructure of zinc thioindate ($ZnIn_2S_4$) thin film-Characteristics. Optik-Int J Light Electron Opt 127: 3858-3861.

189. Veena E, Kasturi VB, Shivakumar GK (2017) Study on structural, optical and electrical properties of spray pyrolysed $Pb_xZn_{1-x}S$ thin films for opto-electronic applications. Optik-Int J Light Electron Opt 144: 528-538.

190. Vidhya SN, Balasundaram ON, Chandramohan M (2015) The effect of annealing temperature on structural, morphological and optical properties of CdZnTe thin films. Optik-Int J Light Electron Opt 126: 5460-5463.

191. Hassanien AS, Akl AA (2016) Effect of Se addition on optical and electrical properties of chalcogenide CdSSe thin films. Superlattices Microstruct 89: 153-169.

192. Mahendran C, Suriyanarayanan N (2015) Influence of mole concentration on nano crystalline Bi-doped $CuInS_2$ thin films with the temperature by chemical spray method. Optik-Int J Light Electron Opt 126: 4237-4242.

193. Ashwini BR, Priyanka UL, Nandu BC (2016) Agitation dependent properties of copper indium diselenide thin films prepared by electrochemical route. Thin Solid Films 615: 366-373.

194. Yogesh SS, Nilesh RT, Ashok UU (2016) Influence of quality of spray solution on the physical properties of spray deposited nanocrystalline MgSe thin films. St. Petersburg Polytechnical Uni J: Phys Math 2: 17-26.

195. Selvakumar C, Venkatachalam T (2015) Structural and optical properties of $CdSnTe_2$ thin films prepared by using closed space vacuum deposition. Mater Sci Semicond Process 39: 686-690.

196. Anwar S, Mishra BK, Shahid A (2016) Optimized substrate temperature range for improved physical properties in spray pyrolysis deposited tin selenide thin films. Mater Chem Phys 175: 118-124.

197. Sahayaraj CAR, Mohan A, Rathesh K, Rajesh S (2017) Structural, optical and electrical properties in indium selenide thin films prepared under nitrogen atmosphere. Mater Today Commun 12: 29-33

198. Azizi S, Rezagholipour H, Ehsani MH (2016) Structural and optical properties of $Cd_{1-x}Zn_xS$ (x=0, 0.4, 0.8 and 1) thin films prepared using the precursor obtained from microwave irradiation processes. Optik- Int J Light Electron Opt 127: 7104-7114.

199. Mohamed JR, Amalraj L (2016) Effect of precursor concentration on physical properties of nebulized spray deposited In_2S_3 thin films. J Asian Ceram Soc 4: 357-366.

200. Logu T, Sankarasubramanian K, Soundarrajan P, Archana J, Hayakawa Y, et al. (2016) Vanadium doping induces surface morphological changes of $CuInS_2$ thin films deposited by chemical spray pyrolysis. J Anal Appl Pyrolysis 122: 230-240.

Published by:

For your own Unlimited Reading and FREE eBooks today visit: https://www.esciencecentral.org/ebooks/

Share this eBook with anyone automatically by selecting any of the options below:

261+
OPEN ACCESS
EBOOKS

10000+
FREE
DOWNLOADS

1+
MILLION
READERS

215+
INTERNATIONAL
EDITORS

1130+
INTERNATIONAL
AUTHORS

To get to know, to discover,
to Publish - this is the destiny.

OMICS International
5716 Corsa Ave, Suite 110, Westlake, Los Angeles, CA 91362-7354, USA,
Ph: +1-650-618-9889, +1-213-204-5002, +1-650-618-1414

Reach us at:
omics.ebooks@omicsonline.org
ebooks@omicsonline.org

please visit: http://www.esciencecentral.org/ebooks/